


## STUDIO DI FASE A2 DELLA MISSIONE GALILEO GALILEI - GG

# FEEP MICROTHRUSTERS SYSTEM - TECHNICAL REPORT

Prepared and  
approved by  
*Approvato da*

  
F. Ceccanti

Date: 28 May 2009  
Data:

## DOCUMENT CHANGE LOG

### Registrazione dei Cambiamenti

ISSUE/ REV. <i>VERSIONE</i>	DATE <i>DATA</i>	TOTAL PAGES <i>NUMERO DI PAGINE</i>	MODIFIED PAGES <i>PAGINE MODIFICATE</i>	REMARKS <i>NOTE</i>
1	28 May 2009	55	All	First issue.

## DISTRIBUTION LIST

*Lista di Distribuzione*

Document Title: <i>Titolo del Documento</i>		FEEP Microthrusters System - Technical Report			
DISTRIBUTION <i>Distribuzione</i>	Type <i>Tipo</i>	Copies <i>Copie</i>	DISTRIBUTION <i>Distribuzione</i>	Type <i>Tipo</i>	Copies <i>Copie</i>
Thales Alenia Space Italia A. Anselmi, G. Sechi	E	1*			
Alta Document Centre	I	1*			
* <i>Electronic Copy</i> <i>E = External</i> <i>I = Internal</i> <i>Copia Elettronica</i> <i>Esterno</i> <i>Interno</i>					

<b>AUTHOR (S)</b> <i>Autore/I</i>  F. Ceccanti		<b>ORGANIZATION (S)</b> <i>Organizzazione/i</i>  Alta S.p.A.		<b>ADDRESS</b> <i>Indirizzo</i>  Alta S.p.A. Via A. Gherardesca 5, 56121 Ospedaletto (PI), Italy Phone: +39 050 985072 - Fax: +39 050 974094	
<b>TITLE</b> <i>Titolo</i>	<b>FEEP Microthrusters System - Technical Report</b>				<b>CI CHECKED:</b> <i>Configurazione</i>  <u>YES</u> NO
<b>CODE</b> <i>Codice</i>  GG.ALT.TN.2003		<b>TYPE OF DOCUMENT</b> <i>Tipo di documento</i>  E		<b>TIME COVERED</b> <i>Tempo coperto</i>  Phase A2	
<b>ISSUE DATE</b> <i>Data del documento</i>  28 May 2009					
<b>PROGRAMME</b> <i>Programma</i>  <u>YES</u> NO		<b>TITLE</b> <i>Titolo</i>  Galileo Galilei - GG		<b>FUNDING ORGANIZATION</b> <i>Organizzazione</i>  ASI	
<b>PROGRAMME ELEMENT</b> <i>Elemento di programma</i>  <u>YES</u> NO		<b>TITLE</b> <i>Titolo</i>  Studio di Fase A2 della missione Galileo Galilei - GG		<b>FUNDING ORGANIZATION</b> <i>Organizzazione</i>  Thales Alenia Space Italia S.p.A. (TAS-I)	
<b>MONITORING PERSON</b> <i>Persona di controllo</i>  Mr. A. Anselmi		<b>CONTRACT No.</b> <i>Contratto no.</i>  GG-SC-ALTA-0918		<b>ADDRESS</b> <i>Indirizzo</i>  Via Saccomuro, 24 00131 - Roma	
<b>ABSTRACT</b> <i>Sommario</i> This document provides the Technical Report on the FEEP Microthrusters System, in the frame of the "Studio di Fase A2 della missione Galileo Galilei - GG". This document summarizes the outcome of the Phase A2 study for the FEEP propulsion system.					
<b>KEY WORDS</b> <i>Parole chiave</i> FEEP, GG, MTS					
<b>AVAILABILITY</b> <i>Disponibilità</i>  <input type="checkbox"/> Approved for public release; distribution is UNLIMITED <input checked="" type="checkbox"/> Approved for LIMITED distribution; no part of this document can be disclosed to third parties without written permission <input type="checkbox"/> CLASSIFIED document for internal use only; no part of this document can be disclosed outside the company					

## CONTENTS

### Indice

<b>1</b>	<b>INTRODUCTION .....</b>	<b>7</b>
1.1	SCOPE .....	7
1.2	PURPOSE .....	7
1.3	APPLICABILITY .....	7
<b>2</b>	<b>THRUSTER TECHNOLOGY DESCRIPTION .....</b>	<b>8</b>
2.1	THE FIELD EMISSION ELECTRIC PROPULSION CONCEPT .....	8
2.2	THE SLIT EMITTER .....	9
2.3	ELECTROSTATIC ACCELERATION IN FEEP .....	10
2.4	COMPARISON OF FEEP WITH OTHER MICRO-PROPULSION TECHNOLOGIES .....	13
<b>3</b>	<b>HERITAGE AND THRUSTER PERFORMANCE .....</b>	<b>14</b>
3.1	CURRENT APPLICATIONS FOR FEEP SYSTEMS .....	14
3.1.1	The FEEP Micro-Propulsion Subsystem (MPS) for Lisa Pathfinder (LPF) .....	14
3.1.2	The Electric Propulsion Subsystem (EPS) for Microscope .....	16
3.2	FP-150 THRUSTER ASSEMBLY DESCRIPTION .....	18
3.3	PCU DESCRIPTION .....	20
3.4	NEUTRALIZER DESCRIPTION .....	22
3.5	THRUSTER PERFORMANCE .....	24
3.5.1	Thrust range .....	24
3.5.2	Thrust resolution .....	25
3.5.3	Thrust noise .....	26
3.5.4	Thrust response time .....	27
3.5.5	Arcing .....	27
3.5.6	Total impulse and specific impulse .....	30
3.5.7	Thruster beam divergence .....	30
3.5.8	Thrust vector errors .....	31
3.5.9	Command frequency .....	33
3.6	OTHER RELEVANT TEST RESULTS AND VERIFICATION ACHIEVEMENTS .....	34
<b>4</b>	<b>THRUSTER REQUIREMENTS FOR GG APPLICATION .....</b>	<b>35</b>
<b>5</b>	<b>PROPULSION SYSTEM ARCHITECTURE AND DESIGN .....</b>	<b>36</b>
5.1	SUBSYSTEM ARCHITECTURE .....	36
5.2	PRODUCT TREE .....	37
5.3	MICRO-THRUSTERS CLUSTER (MTC) DESIGN .....	38
5.3.1	Thruster Assembly description .....	39
5.4	PCU DESIGN .....	40
5.5	NEUTRALIZER ASSEMBLY DESCRIPTION .....	40
<b>6</b>	<b>DESIGN MODIFICATIONS TO MEET GG REQUIREMENTS .....</b>	<b>41</b>
6.1	THRUSTER ASSEMBLY .....	41

6.1.1	Required design change .....	41
6.1.2	Advantages/disadvantages .....	42
6.1.3	Risk mitigation .....	42
6.2	PCU .....	43
6.2.1	Required design change .....	43
6.2.2	Advantages/disadvantages .....	43
6.2.3	Risk mitigation .....	43
<b>7</b>	<b>INTERFACES .....</b>	<b>44</b>
7.1	ELECTRICAL INTERFACES .....	44
7.2	MECHANICAL INTERFACES .....	44
7.3	THERMAL INTERFACES .....	44
<b>8</b>	<b>OPERATIONAL CONSTRAINTS AND LIMITATIONS .....</b>	<b>45</b>
8.1	EMC/ESD.....	45
8.2	CONTAMINATION.....	46
<b>9</b>	<b>DESIGN, DEVELOPMENT AND VERIFICATION PLAN.....</b>	<b>47</b>
9.1	TECHNOLOGY READINESS LEVEL .....	47
9.2	DDV PLAN .....	47
<b>10</b>	<b>DOCUMENTS.....</b>	<b>51</b>
10.1	APPLICABLE DOCUMENTS .....	51
10.2	STANDARDS .....	51
10.3	REFERENCE DOCUMENTS .....	51
<b>11</b>	<b>ACRONYMS.....</b>	<b>52</b>
<b>APPENDIX A</b>	<b>DRAWINGS.....</b>	<b>53</b>
A.1	MTC ENVELOPE DIMENSIONS.....	53
A.2	PCU DIMENSIONS AND MECHANICAL INTERFACES .....	54
A.3	NA DIMENSIONS AND MECHANICAL INTERFACES .....	54
<b>APPENDIX B</b>	<b>.....</b>	<b>55</b>
B.1	MASS BUDGET .....	55
B.2	POWER BUDGET .....	55

# 1 Introduction

## 1.1 Scope

The Galileo Galilei – GG mission has the goal to carry out a test of the *Equivalence Principle* with a sensitivity of a least 1 part over  $10^{17}$ . As a consequence of this “Principle”, all bodies in the gravitational field of a source mass should fall the same, in vacuum, regardless of their mass and composition. This phenomenon goes under the name of “Universality of Free Fall” and is one of the foundations of General Relativity. The need for testing the foundations of General Relativity, hence the Equivalence Principle, is dictated by major current issues such as “dark” matter and “dark” energy, which together account for almost 95% of the Universe and, as the word “dark” indicates, are not understood. The test would be performed in space by a small satellite placed in a near-equatorial, near-circular Earth orbit, for a duration of at least 2 years.

The test is based on a differential accelerometer, made of two test masses of different composition. The test masses are heavy (10 kg each) concentric, co-axial, hollow cylinders. The GG accelerometer is embedded inside the GG payload, called the Pico-Gravity Box (PGB). The largest disturbing accelerations experienced by the accelerometer are due to residual air drag and other non-gravitational forces such as sun and Earth radiation pressure. Such inertial accelerations act on the spacecraft and not on test masses suspended inside it, and are, in principle, the same on both the test bodies. Ideally, common mode effects do not produce any differential signal; in reality, they can only be partially rejected. The approach taken in GG calls for surface accelerations to be partially compensated by a *drag free control system*, and partially abated by the accelerometer’s own common-mode rejection. Drag compensation requires the spacecraft to be equipped with proportional thrusters and a control system to force the spacecraft to follow the motion of an undisturbed test mass inside it at (and close to) the frequency of the signal.

The Field Emission Electric Propulsion (FEED) Microthrusters System (MTS) provides the proportional thrusters required for drag compensation.

This document is the final technical report on the FEED MTS produced in the frame of the phase A2 study of the Galileo Galilei – GG mission.

## 1.2 Purpose

This document provides the outcome of the feasibility study (phase A2) performed to verify the GG mission is feasible using the FEED technology. It provides a description of the technology, including heritage and performance, an analysis of subsystem requirements, a preliminary thruster design solution with evaluation of required modifications vis-à-vis existing design, a preliminary cluster configuration and subsystem architecture, a description of interfaces and operational constraints, and a description of the required development and verification plan for implementation on the GG mission.

## 1.3 Applicability

This document is applicable to GG system level final Phase A2 assessment.

## 2 Thruster Technology Description

### 2.1 The Field Emission Electric Propulsion concept

Field Emission Electric Propulsion (FEED) is an electrostatic propulsion concept based on field ionization of a liquid metal and subsequent acceleration of the ions by a strong electric field.

FEED is currently the object of great interest in the scientific community, due to its unique features: sub- $\mu\text{N}$  to mN thrust range, near instantaneous switch on/switch off capability, and high-resolution throttleability (better than one part in  $10^4$ ), which enables accurate thrust modulation in both continuous and pulsed modes. Presently baseline for scientific missions onboard drag-free satellites, this propulsion system has been also proposed for attitude control and orbit maintenance on commercial small satellites and constellations.

This type of thruster can accelerate a large number of different liquid metals or alloys. The best performance (in terms of thrust efficiency and power-to-thrust ratio) can be obtained using high atomic weight alkali metals, such as Cesium and Rubidium (133 amu for Cs, 85.5 amu for Rb). These propellants have a low ionization potential (3.87 eV for Cs and 4.16 eV for Rb), low melting point (28.7 °C for Cs and 38.9 °C for Rb) and very good wetting capabilities. These features lead to low power losses due to ionization and heating and the capability to use capillary forces for feeding purposes (i.e. no pressurised tanks nor valves are required). Moreover, alkali metals have the lowest attitude to form ionized droplets or multiply-charged ions, thus leading to the best attainable mass efficiency. The actual thrust is produced by exhausting a beam of mainly singly-ionized Cesium or Rubidium atoms, produced by field evaporation at the tip of the *emitter*.

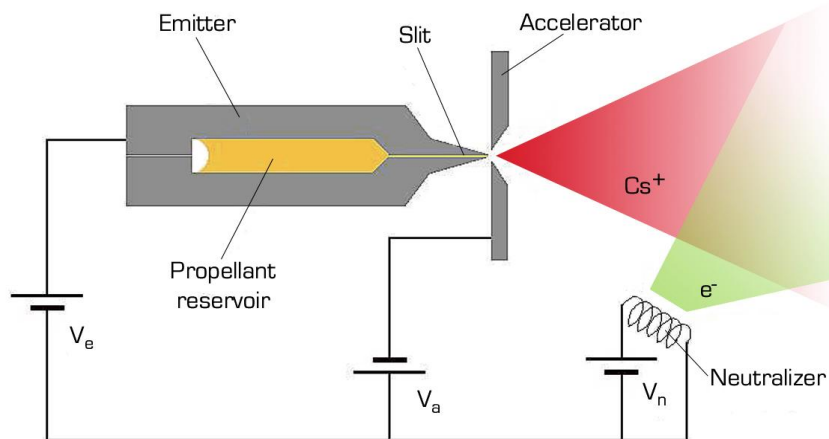


**Figure 2.1: FEED thruster concept.**

An accelerating electrode (*accelerator*) is placed directly in front of the emitter. This electrode consists of a metal plate where two sharp blades are machined. When thrust is required, a strong electric field is generated by the application of a high voltage difference between the emitter and the accelerator. Under this condition, the free surface of the liquid metal enters a regime of local instability, due to the combined effects of the electrostatic force and the surface tension. A series of protruding cusps, or “Taylor cones” are thus created. When the electric field reaches a value in the order of  $10^9$  V/m, the atoms at the tip of the cusps spontaneously ionize and an ion jet is extracted by the electric field, while the electrons are rejected in the bulk of the liquid. An external source of electrons (*neutralizer*) provides negative charges to maintain global electrical neutrality of the spacecraft.



## 2.2 The slit emitter

Liquid Metal Ion Sources (*LMIS*) based on field ionization or field evaporation have been introduced in the late '60s and have quickly become widespread as simple, cheap ion sources for a number of applications. In particular, the use of *LMIS* operated on Ga, In, alkali metals or alloys is standard practice in Secondary Ion Mass Spectrometry (*SIMS*) since the '70s.

While there exist different field emitter configurations, such as the needle, the capillary and slit emitter types, the principle of operation is the same in all cases. In the slit emitter, for example, a liquid metal propellant is fed by capillary forces through a narrow channel. The emitter consists of two identical halves made from hard metal, and clamped or screwed together. A thin-film deposition performed onto one or both of the emitter halves, outlines the desired channel contour and determines channel height (a.k.a. *slit height*, typically 1 to 2  $\mu\text{m}$ ) and channel width (a.k.a. *slit length*, ranging from 1 mm up to about 7 cm, depending on required thrust level).

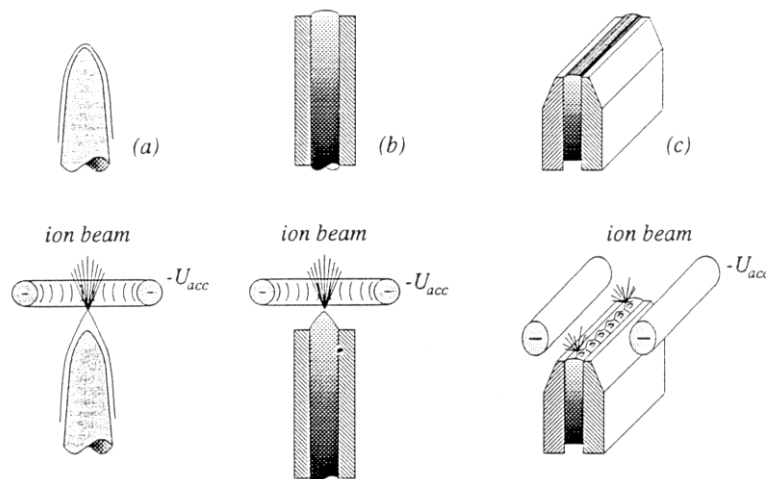


Figure 2.2: FEEP Emitter configurations: Needle (left), Capillary (middle), Slit (right).

The channel ends at the emitter tip, formed by sharp edges that are located opposite a negative, or accelerator, electrode, and separated by a small gap from the emitter tip. An extraction voltage is applied between the two electrodes. The emitter carries a positive potential while the accelerator is at negative potential. The electric field being generated between the emitter and accelerator now acts on the liquid metal propellant.

The narrow slit width not only enables the capillary feed, but, when combined with the sharp channel edges directly opposite the accelerator, also ensures that a high electric field strength is obtained near the slit exit. The liquid metal column, when subjected to this electric field, begins to deform, forming cusps (*Taylor cones*), which protrude from the surface of the liquid. As the liquid cusps form ever sharper cones due to the action of the electric field, the local electric field strength near these cusps intensifies. Once a local electric field strength of about  $10^9$  V/m is reached, electrons are ripped off the metal atoms. These electrons are collected through the liquid metal column by the channel walls, and the positive ions are accelerated away from the liquid through a gap in the negative accelerator electrode by the same electric field that created them.

Slit emitters had been developed to increase the emitting area of the thruster in order to yield higher thrust levels and to avoid the irregular behaviour observed for single emitters. The substantial advantage of slit emitters over stacked needles is in the self-adjusting mechanism governing the

formation and redistribution of emission sites on the liquid metal surface according to the operating parameters; in a stacked-needle array, on the contrary, the Taylor cones can only exist on the fixed tips, which pre-configure a geometrical arrangement that can only be consistent with one particular operating condition.

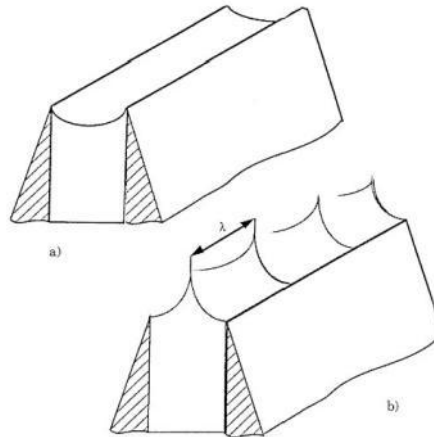


**Figure 2.3: Taylor Cones Formation in a Slit Emitter.**

Slit emitters with a wide variety of slit widths (between 2 mm and 7 cm) have been fabricated; these devices, spanning a thrust range from 0.1  $\mu\text{N}$  to 2 mN, have been operated with either cesium or rubidium. The two pictures below show two of Alta's early FEEP thrusters during testing, with the characteristic plume colours: blue for cesium and red for rubidium.



**Figure 2.4: Alta's FEEP thrusters firing with Cs (left) and Rb (right) propellants.**

More recently, the development focused on the overlapping requirements for the Microscope and the Lisa Pathfinder missions. The outcome of such development is Alta's FP-150 thruster, which is described in sect. 3.2 below.

## 2.3 Electrostatic acceleration in FEEP

The essential elements of the FEEP thruster are shown in the following Figure 2.5. Such scheme resembles that of a one-dimensional electrostatic accelerator, as described in Jahn<sup>1</sup>, and is in fact equivalent (albeit simpler) to that of a gridded ion thruster, except for the means of ion generation and extraction.

<sup>1</sup> R. G. Jahn, *Physics of Electric Propulsion*, McGraw-Hill, 1968.

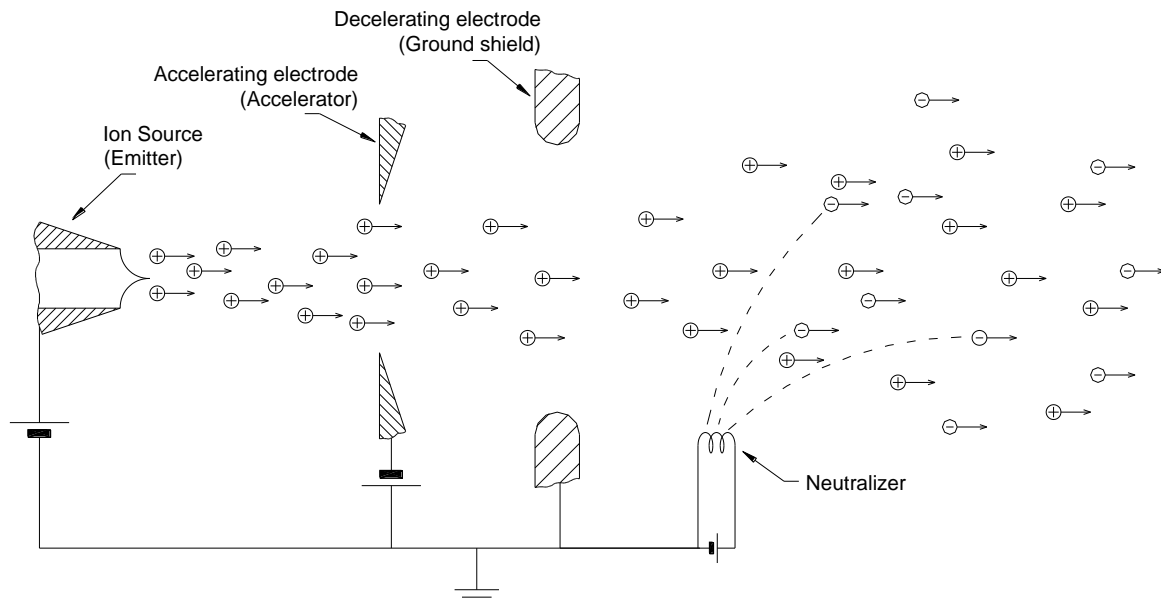


**Figure 2.5: Schematic electric diagram of the FEEP thruster.**

A stream of ions is liberated from the liquid metal meniscus in the *emitter* slit, by the field emission principle described in the previous section. The beam is then accelerated by the same electric field established between the positive emitter and the negative accelerating electrode (*accelerator*). The beam exits the accelerator with a velocity determined by the total potential drop between the emitter and the accelerator, and by the charge-to-mass ratio of the generated ions (see Figure 2.7).

After exiting the accelerator, the beam is decelerated by a potential rise, being the outer shield of the thruster usually grounded to the S/C potential. Subsequently, a stream of electrons joins the ion stream, producing a beam of zero net charge. The neutralizer mainly provides overall charge compensation to the S/C, keeping the S/C potential close to equilibrium with ambient plasma. The effective potential difference between S/C and ambient plasma depends on the effectiveness of the neutralizer. In active electron sources, such as electron guns, the emitted electron current must be exactly matched to that of the ion source. In a passive device, such as a thermionic neutralizer, the amount of electrons that are extracted from the neutralizer is proportional to the voltage difference between the S/C and the ambient plasma. The S/C potential then is brought to a small negative offset, enough to extract the exact amount of electrons to reach equilibrium. The more the electron source is effective (i.e. electrons can be extracted easily), the smaller is the equilibrium offset.

The potential rise beyond the accelerator has two main effects:

- it slows the exiting ions, therefore reducing  $I_{sp}$  and power-to-thrust ratio (at first instance, power-to-thrust ratio is proportional to exit velocity);
- it prevents free electrons from entering the accelerator-emitter gap, where they would be accelerated towards the emitter, with several negative drawbacks (emitter tip would be heated by electron bombardment, with ensuing increase in propellant evaporation).

As it can be seen by the following figures, the final exit velocity ( $v_e$ ), and therefore  $I_{sp}$ , is ultimately determined by the potential at the emitter electrode (*emitter voltage*,  $V_e$ ). On the other hand, for the extraction mechanism described in section 2.1, the mass flow is determined by the electric field at the emitter tip, which is proportional to the *total voltage* difference, i.e.  $V_e - V_a$ .

As the thrust is proportional to both exit velocity and mass flow, operational parameters of FEEP (e.g. power-to-thrust ratio, Isp vs. thrust curve) can be modified to some extent by properly adjusting the voltage values.

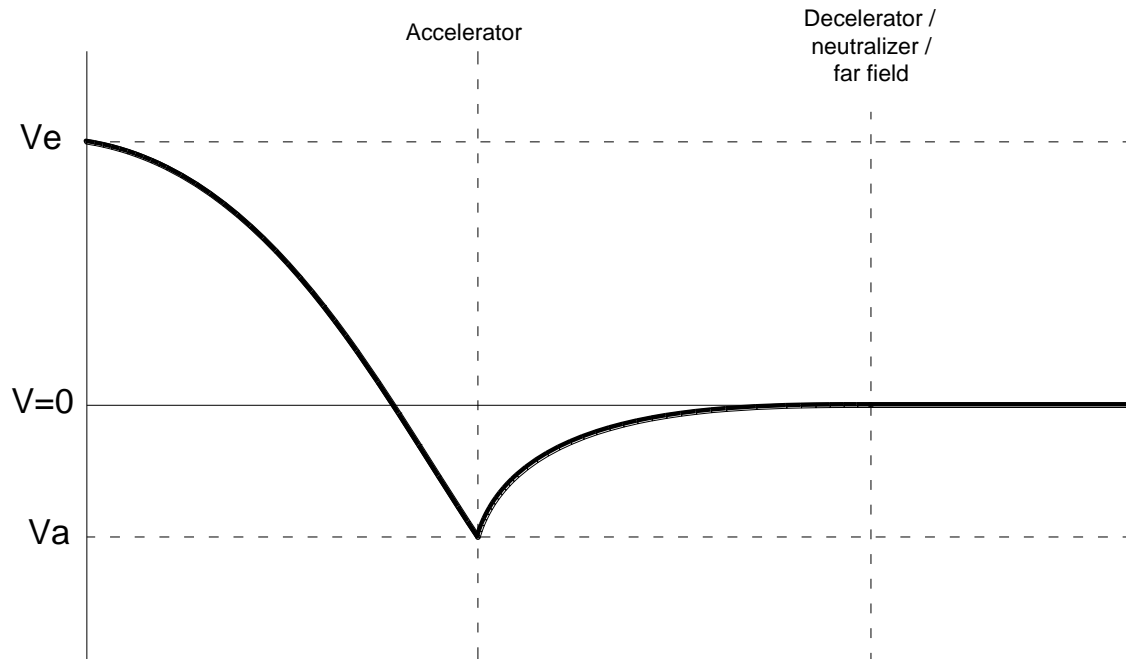


Figure 2.6: Potential profile.

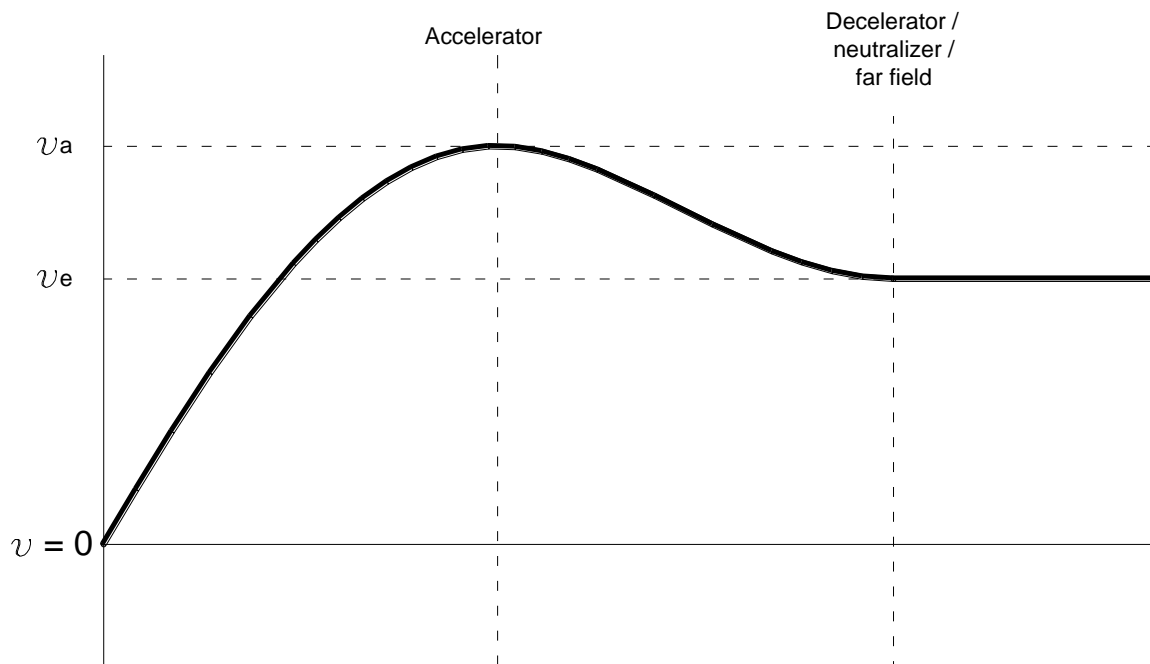


Figure 2.7: Velocity profile.

## 2.4 Comparison of FEED with other micro-propulsion technologies

The FEED technology has unique features making it the choice whenever ultimate performance in terms of thrust resolution and throttleability, low noise level, and thrust step response is requested.

It has no moving parts during operation, which means that mechanical disturbance is reduced to a minimum.

Its very high specific impulse ( $> 3000$  s) makes the mass consumption during the mission very low. This can be crucial when it is desirable to minimize variation of S/C mass and inertia properties during the mission.

Being an ion thruster, the thrust behaviour can be characterized in terms of electrical parameters, and in-flight analysis of thruster performance can be based on real-time telemetries.

Characterization of the ion plume allows assessment of thrust vector with thrust and time (including lateral force noise).

An ion thruster (with its neutralizer) also provides an effective mean to avoid S/C charging, creating a sort of plasma bridge between the S/C and the space plasma, thus minimizing disturbances from surface charge accumulation. Furthermore, DC and AC magnetic performance can be optimized due to the absence of valves and solenoids.

Finally, the proposed cesium-fed, slit-emitter type FEED technology is being fully demonstrated and qualified in the frame of ESA's Lisa Pathfinder programme, making it available for future users as an almost "off-the-shelf" technology.

### 3 Heritage and thruster performance

#### 3.1 Current applications for FEPP systems

The FEPP technology is, at present, the micro propulsion baseline for two European drag-free missions: ESA's Lisa Pathfinder and CNES' Microscope.

##### 3.1.1 The FEPP Micro-Propulsion Subsystem (MPS) for Lisa Pathfinder (LPF)

Lisa Pathfinder is an ESA mission belonging to the SMART family. The primary aim of the SMART missions is to flight test the technologies needed for future, Cornerstone missions; the challenge is to launch and operate a satellite to validate critical new technologies within strictly limited funding resources and stringent planning constraints. This can only be achieved by extensive use of the technical expertise gained by Industry and the Agency in previous projects. LISA Pathfinder will address the technology needs of LISA (Laser Interferometer Space Antenna), which will entail co-operation between ESA and NASA. The primary objective of LISA is the detection of gravitational waves in the one millihertz to one hundred millihertz band, which are predicted by general relativity to be emitted by distant galactic sources such as compact binaries. LISA will consist of three spacecraft flying in a quasi-equilateral triangular formation, separated by five million kilometers, in a trailing Earth orbit of some twenty degrees.

The LISA Pathfinder mission is required to place a spacecraft into an orbit compatible with the technology demonstration requirements. The technology demonstration package of LISA Pathfinder will consist of two payloads (the LISA Technology Package – LTP – developed by European institutes and industry, and the Disturbance Reduction System (DRS) provided by NASA's Jet Propulsion Laboratory) and, as part of the platform, the Micro-Propulsion Subsystem (MPS) and the Drag-Free and Attitude Control Software (DFACS). The industry responsible for the Lisa Pathfinder platform is Astrium Ltd; Galileo Avionica is the appointed subcontractor for the Micro-Propulsion Subsystem, which will be based on Field Emission Electric Propulsion (FEPP) technology. As subcontractors to Galileo Avionica, Alta is developing the Slit FEPP Cluster Assembly and Thales Alenia Space Italia is developing the Neutralizer Assembly.

The FEPP Micro Propulsion Subsystem for Lisa Pathfinder is made of:

- 3 FEPP Cluster Assemblies (FCA);
- 3 Neutralizer Assemblies (NA), made of two neutralizer units (NU) each;
- 3 Power Conditioning Units (PCU).

In turn, each FCA is made of:

- 4 Thruster Assemblies (TA);
- the supporting and interface structure (Thruster Cluster Structure, TCS);
- the required thermal control hardware;
- the required harness, including low voltage connectors and high voltage flying leads.

Each PCU is capable of controlling 4 thrusters (i.e. one FCA) and one neutralizer unit at once. The neutralizer units are operated in cold redundancy, with just one active NU (out of two) per each NA. The FCAs are placed on three locations on the external panels of the Lisa PF spacecraft, according to Figure 3.1. One PCU is placed close to each FCA, on the internal side of the same panel, while the three neutralizer assemblies are placed on three different panels, which do not carry thrusters. The thruster clusters and neutralizer assemblies are mounted on the external side of the panel, while the PCUs are mounted on the internal side.

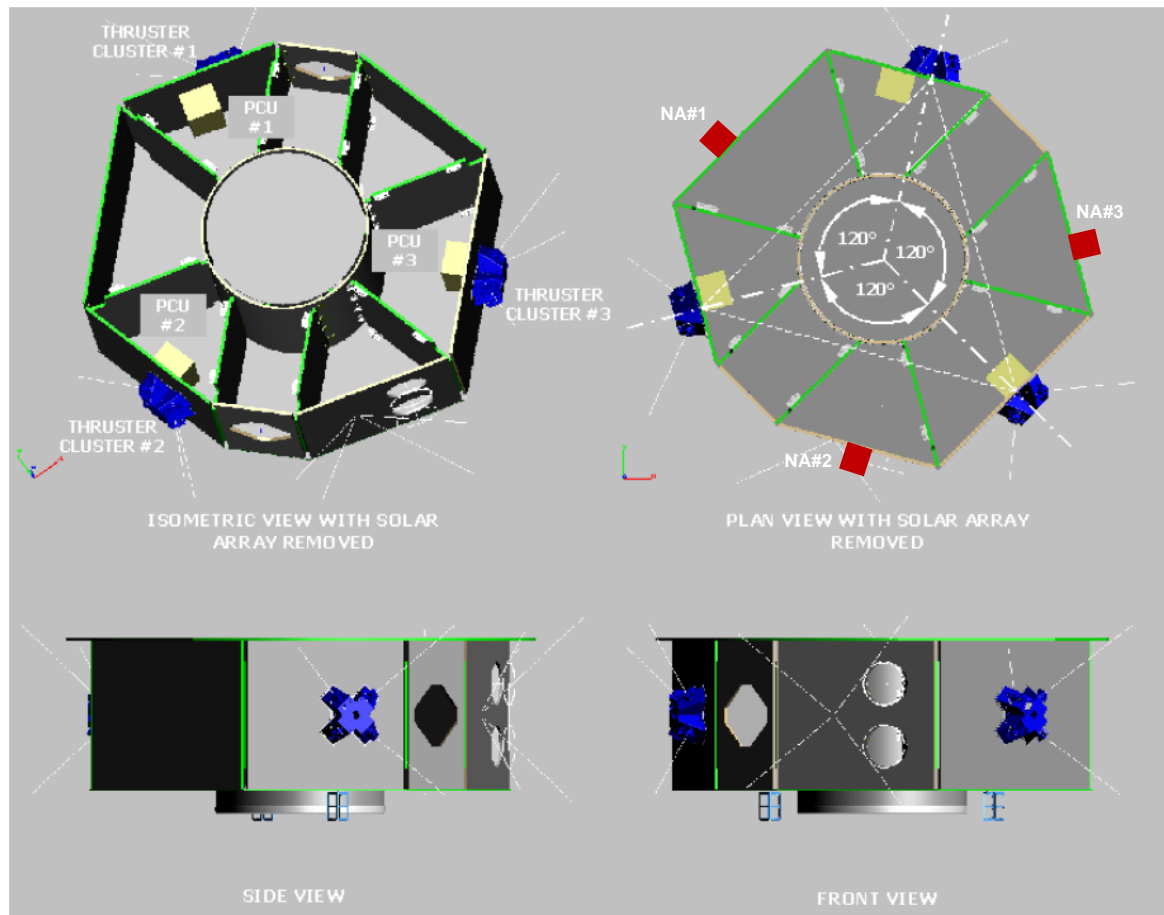


**Figure 3.1: FCA, NA and PCU location on the Lisa Pathfinder spacecraft.**

The following figures show the layout of the FCA and thrust vector directions.

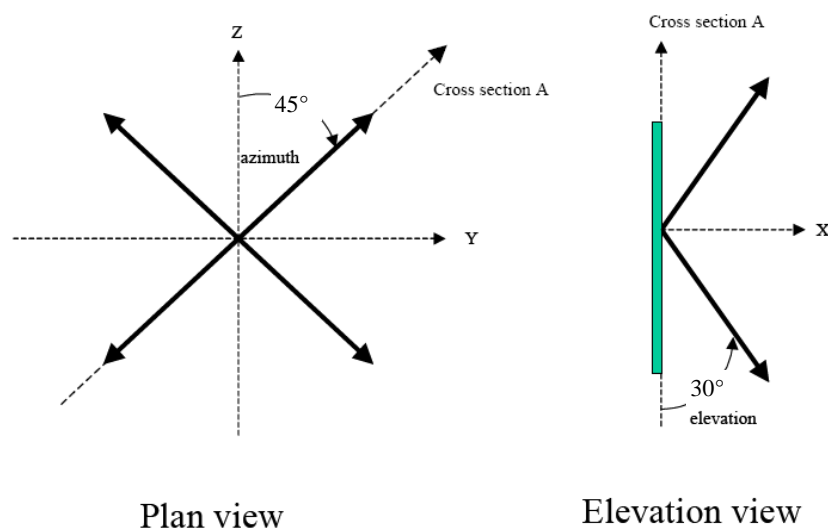


**Figure 3.2: FCA thrust vector angles.**



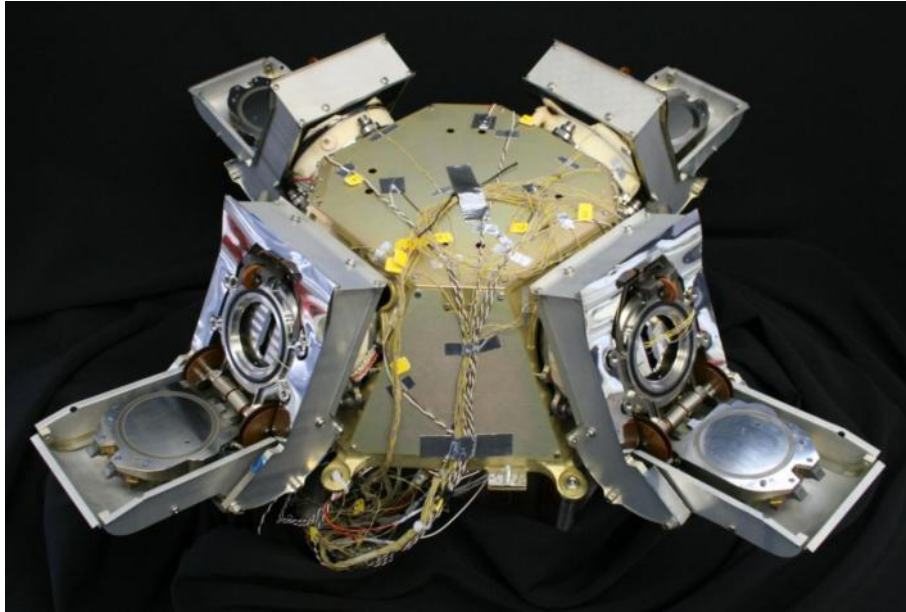


Figure 3.3: FCA, thrusters in open (flight) configuration, no MLI shown.

### 3.1.2 The Electric Propulsion Subsystem (EPS) for Microscope

Microscope is a space fundamental physics mission initiated by the French ONERA institute, and approved by the French space agency (CNES) Scientific Program Committee in the frame of the scientific missions exploiting CNES' microsatellite product line. The scientific objective of the mission is to test Galileo Galilei's Equivalence Principle with an accuracy of  $10^{-15}$ , i.e. about two orders of magnitude better than the accuracy of the present on-ground experiments. In other words, the mission has the same objective of GG; but its accuracy target is two orders of magnitude worse than GG itself.

The instrument is composed of two differential electrostatic accelerometers, each including two cylindrical and concentric test masses. The masses are made of the same material (platinum) for the first accelerometer which is dedicated to assess the accuracy of the experiment, while the masses are made of platinum and titanium for the second accelerometer exploited to test the Equivalence Principle. The attitude as well as the atmospheric and thermal drag of the satellite are actively controlled in such a way that the satellite follows the two test masses in their pure gravitational motion. The test-mass motions, with respect to highly stable silica instrument frame, are also servo-controlled using very accurate capacitive position sensing and electrostatic actuators. The relative position of the two masses is thus maintained motionless and the fine measurement of the control force leads to the test of the Equivalence Principle with the expected accuracy.

The satellite drag compensation and attitude control involves FEEP thrusters. In the frame of a joint ESA-CNES cooperation, ESA will procure the FEEP Electric Propulsion Subsystem for the Microscope mission. Alta is the appointed prime contractor for the FEEP Electric Propulsion Subsystem, having Galileo Avionica as a subcontractor for the FEEP Power Processing and Control Unit and Thales Alenia Space Italia as a subcontractor for the Neutralizer Units.

The Electric Propulsion Subsystem for Microscope is made of four Electric Propulsion Subsystem Assemblies (EPSA).



In turn, each EPSA is made of:

- 3 Thruster Assemblies (TA);
- two Neutralizer Units;
- one Power Processing and Control Unit (PPCU);
- the supporting and interface structure;
- the required thermal control hardware;
- the required harness, including low voltage connectors and integrated high voltage connections.

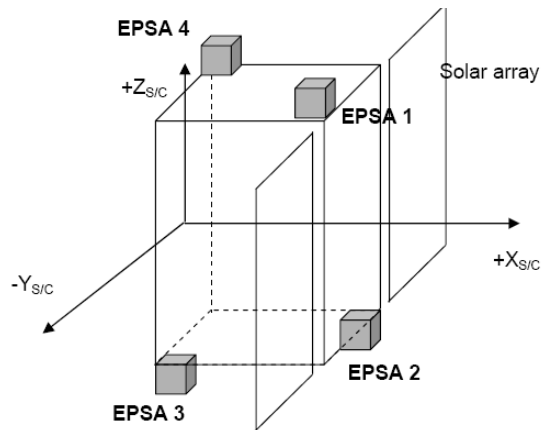
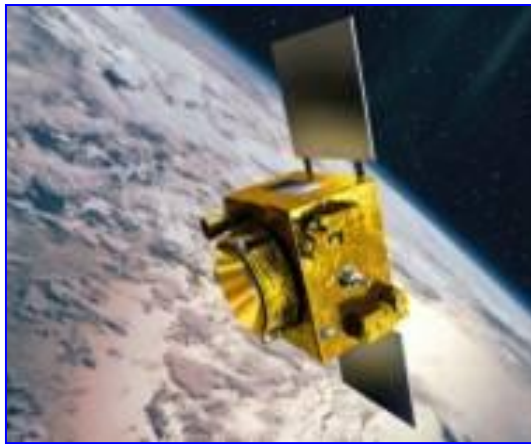
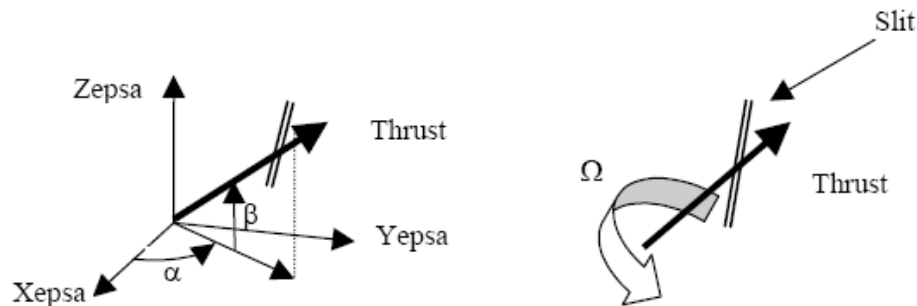


Figure 3.4: Microscope spacecraft (left), and location of EPSAs on the S/C (right).

The EPSAs are placed at four corners of the Microscope spacecraft structure, on two opposing panels, according to Figure 3.4. EPSAs electrical interfaces are basically one power connector and one data connector. HV generation and HV wires routing is done internally to the EPSA. Each EPSA embeds its own PPCU, controlling the 3 EPSA thrusters and the 2 EPSA neutralizers. The nominal operative mode is with all thrusters and one neutralizer active for each EPSA. The following figures show the layout of the EPSA and thrust vector directions.



Thruster	Alpha (deg.)	Beta (deg.)	Omega (deg.)
A	-148	25	91
B	63	25	-78
C	-33	-30	57

Figure 3.5: EPSA thrust vector angles.

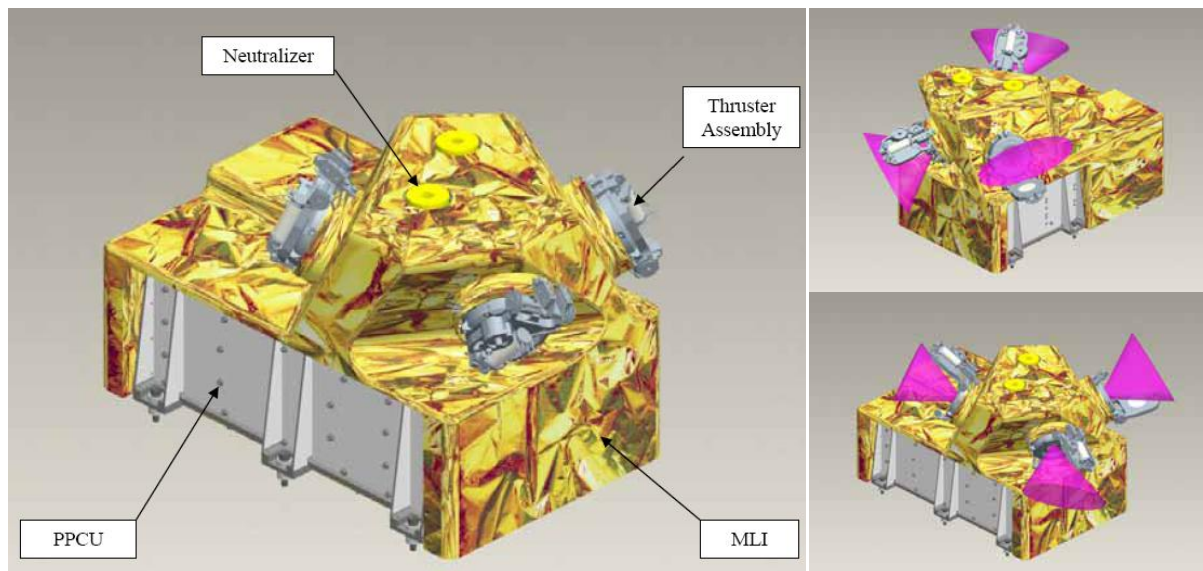


**Figure 3.6: EPSA layout. Launch configuration (closed lids, left), and in-flight configuration (with thrusters firing, right).**

### 3.2 FP-150 Thruster Assembly description

One single product, the FP-150 Thruster Assembly (TA), is being developed for both the Lisa Pathfinder and the Microscope programmes. The only difference, at thruster level, is the external thermal shields that are needed for Lisa Pathfinder, due to the worse thermal environment. The mass of the thruster assembly, excluding the thermal shields, is about 1.5 kg, including about 90 grams of cesium propellant.

The main sub-assemblies of the TA are:

- Thruster Unit;
- Lid Opening Mechanism (LOM);
- Propellant Reservoir (Tank);
- Heater Assembly.

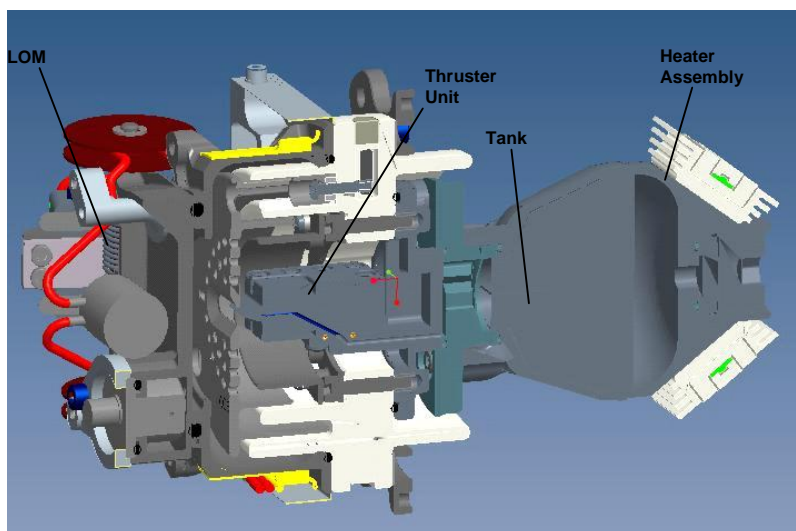


**Figure 3.7: TA Cross Section.**

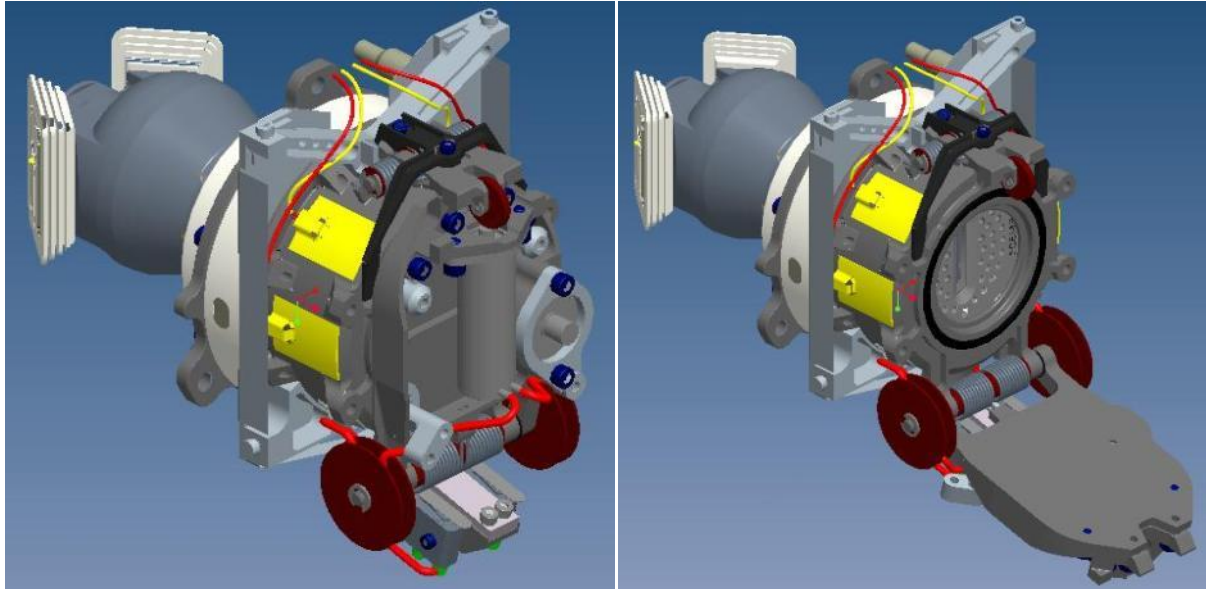


**Figure 3.8: Thruster Assembly layout with lid closed (left) and with lid open (right)**

The following is a brief description of the TA operation and functions:

- The tank is a closed reservoir. It is sealed by two metal gaskets and one welded rupture disk (Tank Sealing Device, TSD), which is a notched Inconel membrane. The TSD is designed, qualified and accepted (by batch testing) to break within a certain pressure (about 45 bar). The tank is filled with a well calibrated cesium amount (function of actual volume of each single tank), in order to have the cesium filling the whole tank internal volume at a certain temperature ("Filling Temperature"), with an accuracy of  $\pm 5$  °C. The filling temperature is selected as a function of on-ground and LEOP environmental constraints, in order to avoid pressurization of the tank during such phases. For Lisa Pathfinder, the selected filling temperature is about 65 °C.
- The Thruster Unit, composed of the thruster electrodes and the main ceramic insulator, after having been thoroughly cleaned and baked-out during the assembly phase, is kept in dry, inert argon atmosphere during all ground phases by the sealed container/LOM.
- Once in orbit, the first operation for thruster activation is LOM opening: a space-qualified paraffin actuator releases a latch, and the cover lid opens under the torque exerted by preloaded springs. The thruster is then allowed to vent for some time (2 days typically) to release the storage argon and eventual moisture residuals.
- After that phase, cesium is allowed to exit the reservoir: by heating up the tank (using the dedicated Heater Assemblies) cesium expands until it pressurizes the tank to TSD rupture pressure. Rupture is achieved within 15 to 25 °C above tank filling temperature.
- Further heating of the tank (up to  $45 \pm 5$  °C above filling temperature in current design) allows cesium to fill all the pipeline leading to the emitter, and to be forced inside the emitter duct up to emitter tip. During this phase (called "Forced Priming Procedure") temperature is increased very slowly by the PCU, while electrodes voltage is kept at high values, so that, as soon as the propellant reaches the tip, emission is started and procedure is interrupted.
- After this phase, heater assemblies are kept at a certain preset temperature, that ensures cesium is liquid whatever the external thermal environment conditions (sun or shadow/eclipse) and the thruster is operated controlling the thrust level by varying the emitter voltage (closed loop thrust control is performed by PCU).

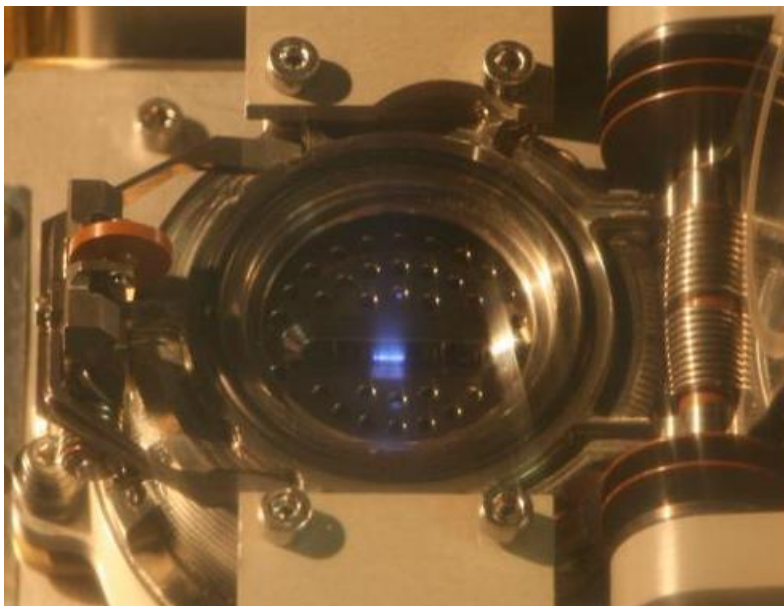


**Figure 3.9: Thruster Assembly firing immediately after successful priming procedure.  
("Neutralization Test", ESTEC Electric Propulsion Laboratory, April 2009.)**

### 3.3 PCU description

The developed power control units for Lisa Pathfinder and Microscope differ in the power bus and telecommand/telemetry interfaces<sup>1</sup>, and in number of commanded thrusters (3 for Microscope and 4 for LPF for each PCU unit), while the high voltage boards, the functions and the architecture are the same for the two programmes. The PCU for Lisa Pathfinder, which is almost identical to the one proposed for GG, is described below.

The PCU performs control and power management of four FEEP thrusters to provide a thrust level ranging from 0.1  $\mu\text{N}$  to 150  $\mu\text{N}$  with very high resolution and low noise. To this purpose, the PCU allocates 8 High Voltage generators (up to +12 kV for emitter and -1.7 kV for accelerator) with voltage/current control and on-board calibration capability. Emitter voltage regulation is varying from 2.5 kV to 12 kV at very low current levels (from 0.5  $\mu\text{A}$  to 1 mA). In addition the PCU includes 8 low voltage power supplies for propellant heating (thermal control) and dedicated power supplies for release of the lid opening mechanism.

The PCU also performs control and power management of two thermionic neutralisers (one main and one in cold redundancy), which are necessary to avoid spacecraft charging due to FEEP operation. To this purpose, the PCU includes 6 low voltage power supplies with voltage/current control and on-board calibration capability.

Single point failure tolerant architecture guarantees operation of three thrusters and one neutraliser in case of any single failure at PCU level. This configuration is also applied to the spacecraft interfaces. To support this function the system has to provide two Main Bus and two command/telemetry interface lines operating in cold redundancy.

PCU main block diagram is shown in Figure 3.10.

<sup>1</sup> Lisa Pathfinder: regulated 28 V bus, MIL-1553 TC/TM I/F. Microscope: non-regulated 22-37 V bus, RS-422 interface.



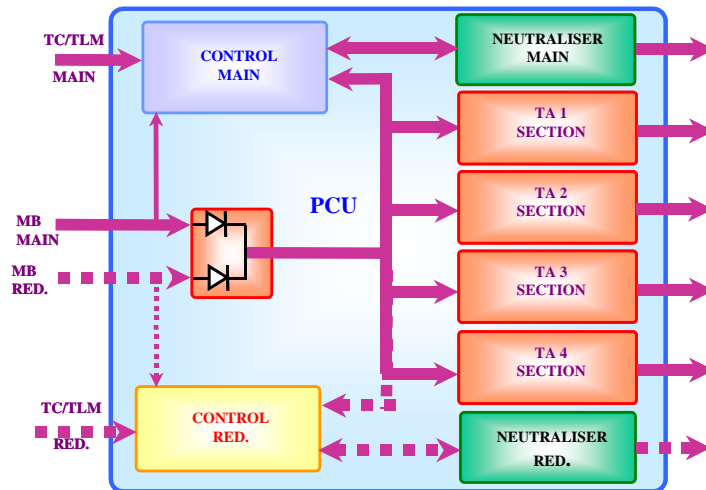


Figure 3.10: PCU block diagram.

The following internal modules are allocated inside the PCU:

- Four Power Boards; each containing one complete FEEP power supply section (High Voltage and Low voltage sections);
- Two Control Boards; each one containing the logic and neutraliser sections (main and red. respectively)
- One Mother Board for cross strapping function among all the above modules.

The PCU is capable to operate with regulated main bus voltage (i.e. 28V) with capability to support operation also in an unregulated main bus scenario (i.e. from 20.5 to 29 Volts) since allocates dedicated dc/dc regulators on each main function directly connected to the main bus line.

As far as command and telemetry (TC/TM) interface is concerned, the amount of signals required to manage FEEP thrusters and neutralisers (for monitoring, in-flight calibration and failure detection) lead to have tens of commands and telemetries; this impose to use serial interfaces for their managing from/to the On-Board Computer (OBC). MIL-STD-1553 Data Bus interface (asper Lisa Pathfinder design) is proposed.

A Field Programmable Gate Array (FPGA) is used to build the complete logic section; it is a space-qualified Actel FPGA with Rad-Hard total dose capability to sustain mission total dose and triple voting logic implementation for Single Event Phenomena mitigation. The logic section is aiming to manage the status of the whole cluster of thrusters (up to 4) according to a defined and reliable operational modes.

The protection level implemented at PCU side has been reduced to the minimum: each parameter exceeding the “nominal and safe” value that can lead to fault condition shall be managed at system level (i.e. OBC) in order to reduce any interruption of FEEP thrusters operation. The only protections that are autonomously managed by the PCU are those necessary to avoid failure propagation in the subsystem and, as a consequence, then propagating to the spacecraft (e.g. Main Bus under-voltage protection).

The mechanical structure of the PCU is constituted of a box made of Aluminium Alloy 7075: one base plate, one front wall, one rear wall and a C-shape cover, joined together with stainless steel screws.

The PCU is fixed to the inside of satellite panels by means of six mounting feet providing adequate means of sustaining the specified environment (both mechanical and thermal).

Figure 3.11 shows the PCU mechanical/architectural configuration (one control board, one power board and the mother board with mechanical structure are shown). The PCU architecture provides also a physical segregation between each FEFP thruster section.



**Figure 3.11: PCU box opened.**

### 3.4 Neutralizer description

The Neutralizer Unit for both the Lisa Pathfinder and the Microscope missions is produced by TAS-I (Florence). The NU is a moderately high perveance electron gun; the electrons source is a thermionic cathode, made of porous tungsten impregnated with barium, calcium, aluminium and scandium oxides.

The following pictures show the Neutralizer Unit and the Neutralizer Assembly, made of two Units mounted together on a common supporting structure.

Further details on Neutralizer description can be found in [RD 5].

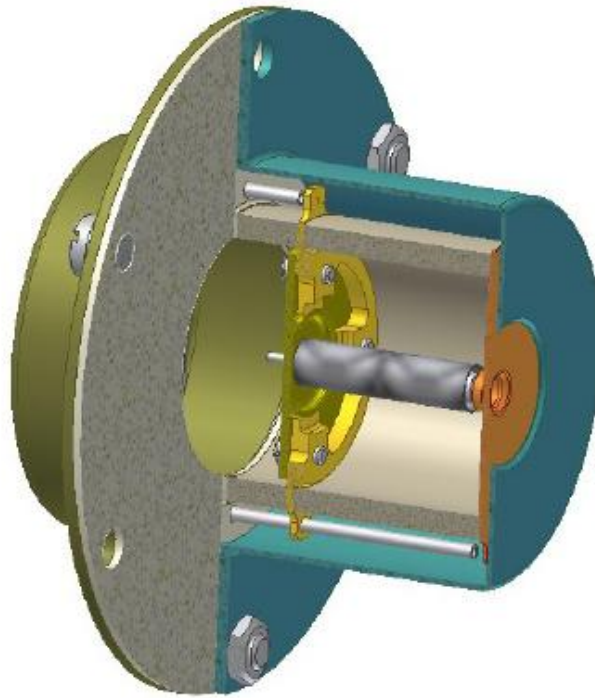


Figure 3.12: Neutralizer Unit 3D view (section).

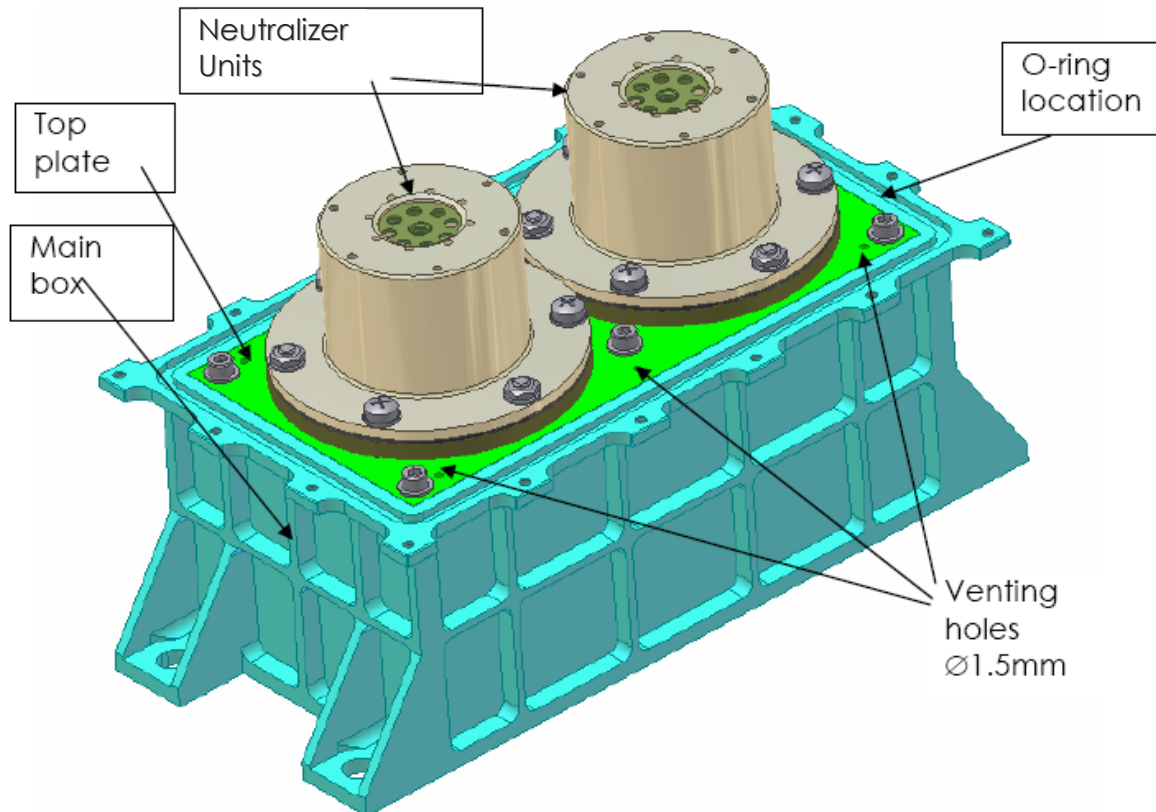


Figure 3.13: Neutralizer Assembly 3D view.

### 3.5 Thruster performance

The following sections provide a summary of the performance of the FEPP system (i.e. thruster + PCU coupled behaviour), with reference to test data as recorded during the various tests performed in the frame of the Lisa Pathfinder development.

#### 3.5.1 Thrust range

Thrust can be commanded in the range 0.05 to 204.8  $\mu\text{N}$  with 12 bit resolution (i.e. 4096 steps of 0.05  $\mu\text{N}$  each). Thruster is designed for the range 0.3 to 150  $\mu\text{N}$ , and effective operation throughout this range was verified during various priming tests and endurance tests (i.e. in all recently performed tests).

Minimum thrust target, 0.1  $\mu\text{N}$ , was verified during Thruster Assembly Priming Test (TAPT) No. 3. It is noted, however, that thrust control in the very low thrust region tends to be quite unstable, possibly due to switching on and off of some of the few active Taylor cones. To get better thrust stability at low thrust (as well as better command response), it is recommended to use the thruster with a minimum thrust level (bias) of 0.5  $\mu\text{N}$  or higher. For reference, the Lisa Pathfinder DFACS considers a minimum thrust of 4  $\mu\text{N}$  during science mode operation.

*Note: The maximum thrust reached during the test EVT#4 was 540  $\mu\text{N}$ , showing the thruster operates with a large margin with respect to its effective maximum thrust capabilities.*

During the DTM test (on TAS-I nanobalance facility), direct measurement of the 0-200  $\mu\text{N}$  thrust range was also performed, providing updated factors for correlation between thrust and electrical parameters.

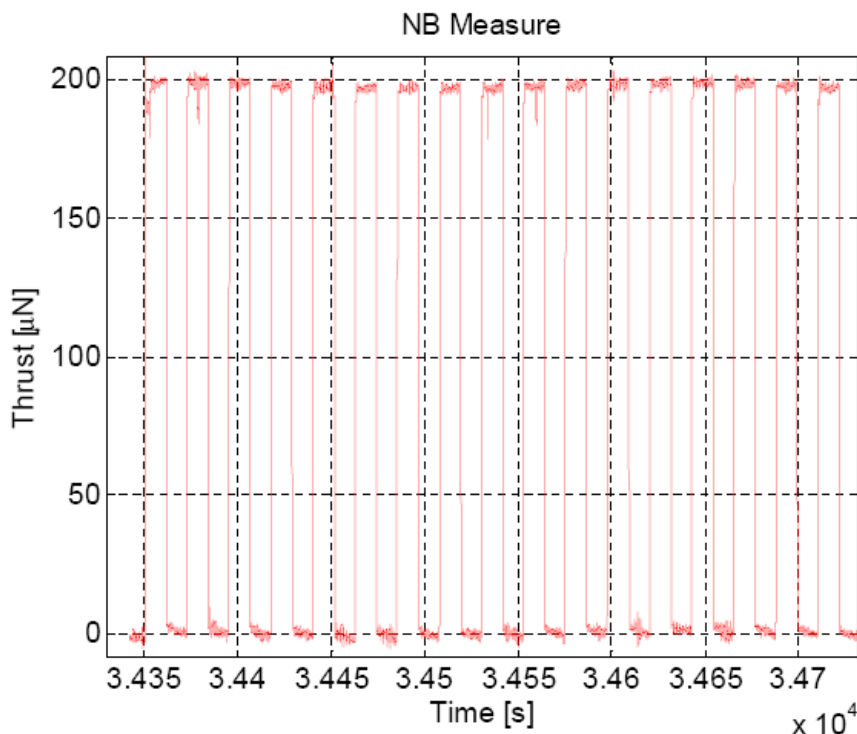


Figure 3.14: Test of thrust range during DTM test.



### 3.5.2 Thrust resolution

Thrust resolution was verified during coupled TA-PCU testing. The following plots show the required resolution is driven by PCU control (1 LSB error = 50 nN), and the thruster easily follows PCU command. Resolution was also measured during Direct Thrust Measurement Test (on TAS-I nanobalance).

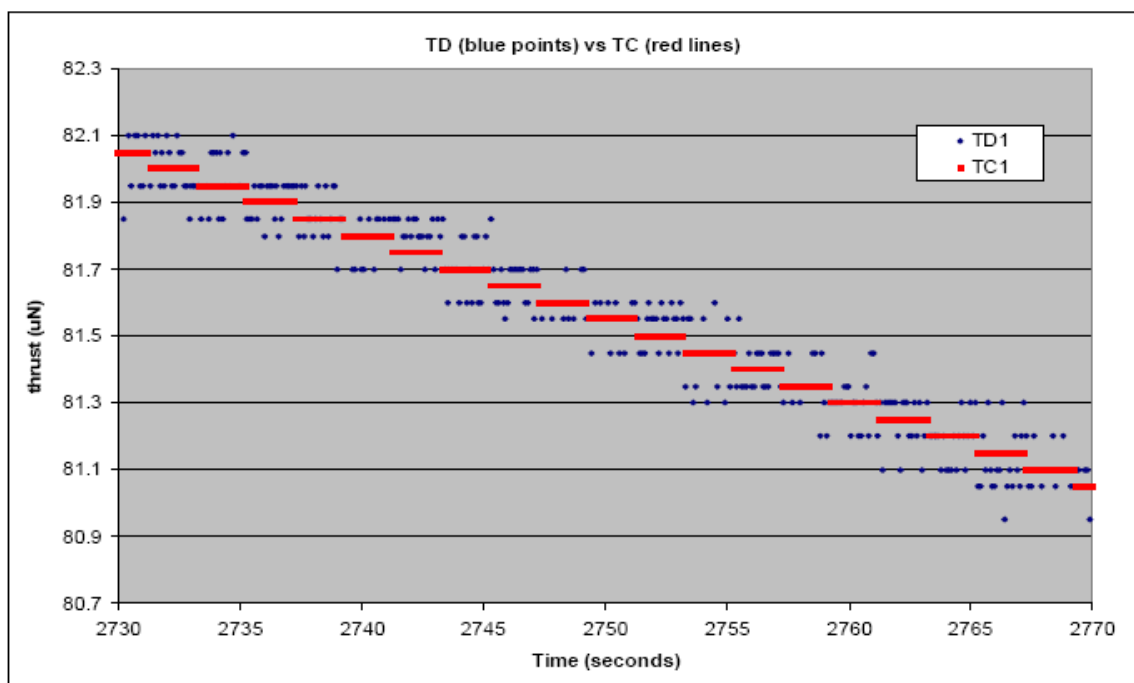


Figure 3.15: Delivered thrust (TD) and commanded thrust (TC).

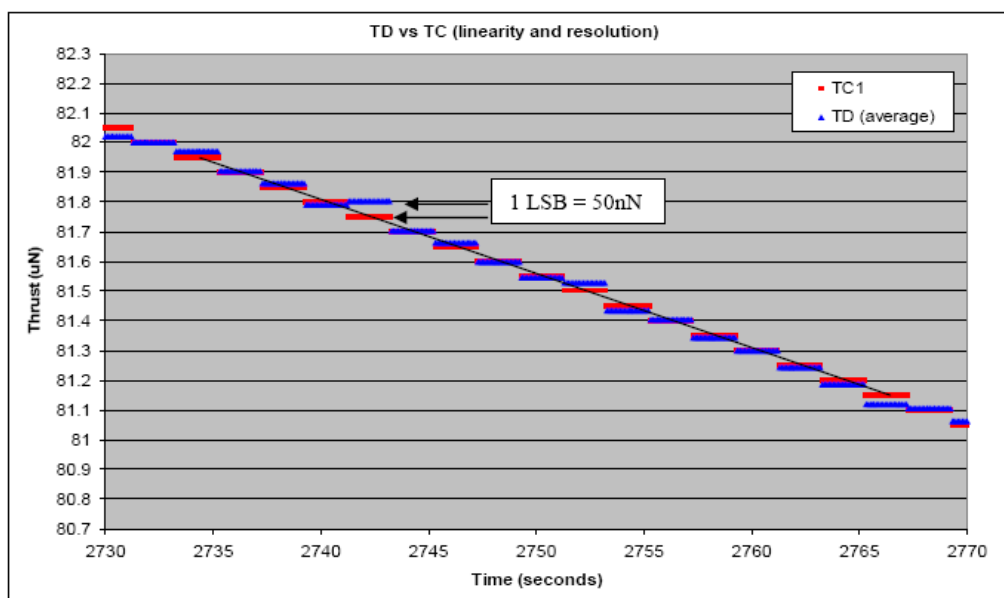


Figure 3.16: Averaged delivered thrust (TD average) and commanded thrust (TC).

### 3.5.3 Thrust noise

Thrust noise measurement (based on electrical parameters) was carried out in TAPT#2. Figure 3.17 shows the noise PSD value at 100  $\mu\text{N}$ , calculated by suppressing the sparks (i.e. artificially putting thrust level equal to 100  $\mu\text{N}$  during sparks). This provides the noise due to thrust control only. Spark effects are treated separately (see sect. 0).

Direct measurement of noise (including sparks effect) was then performed during the Direct Thrust Measurement (DTM#2) test on TAS-I (Turin) nanobalance facility. The test highlighted that thrust noise from the FEEP system (thruster + PCU) is below the nanobalance detection threshold (which, in turn, is lower than 1  $\mu\text{N}/\sqrt{\text{Hz}}$ ), confirming the results of the indirect measurements.

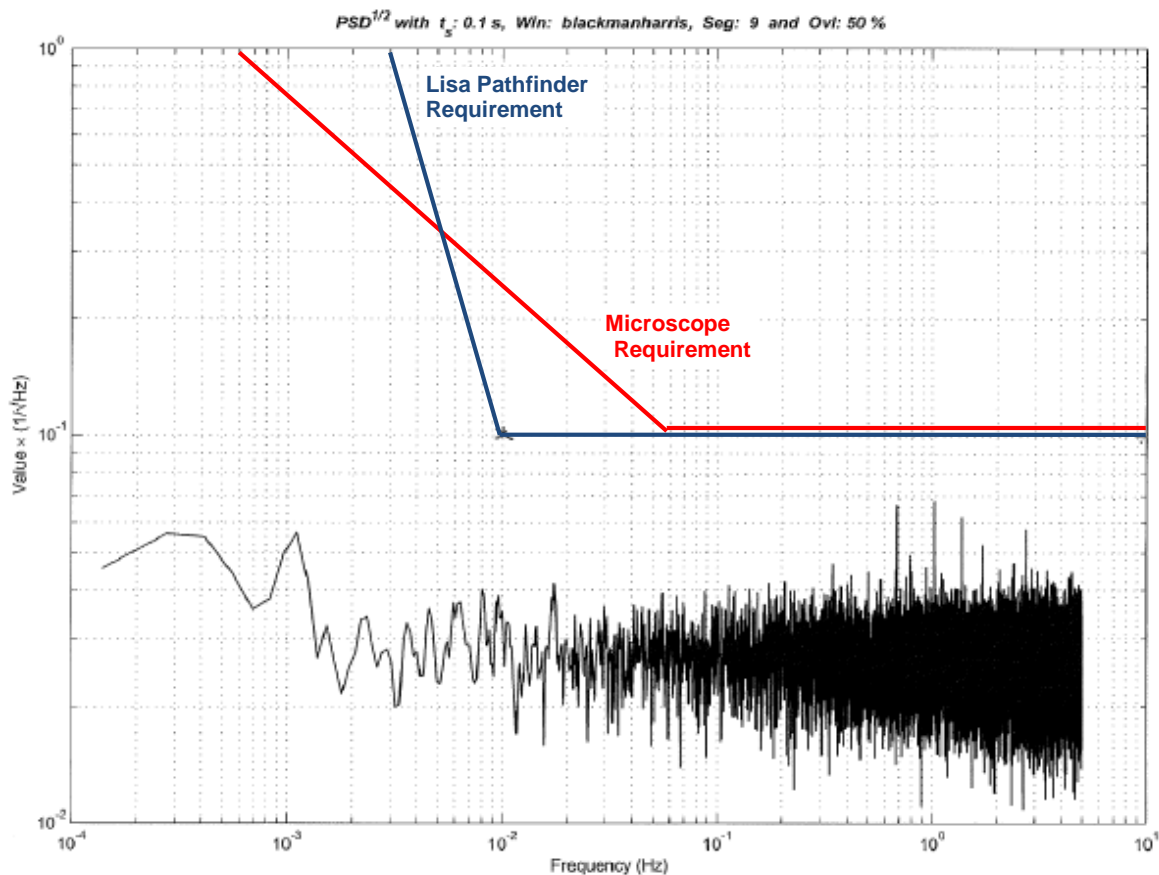


Figure 3.17: Thrust noise at 100  $\mu\text{N}$ , purged of sparking effects.

### 3.5.4 Thrust response time

Thrust response was verified with PCU during TAPT#2. The relevant results are reported below.

Transient	Requirement		Measured (*)	Compliance
from 0 to 150 $\mu$ N	10 s	FEE-1982	0.27 s	Yes
from 0 to 150 $\mu$ N	3.3 $\mu$ N	FEE-864	3 $\mu$ N	Yes
from 150 to 0 $\mu$ N	10 s	FEE-1982	0.25 s	Yes
0.3 to 30.3 $\mu$ N	190 ms	FEE-106	150 ms	Yes
30.3 to 0.3 $\mu$ N	190 ms	FEE-106	100 ms	Yes
4 to 34 $\mu$ N	190 ms	FEE-106	120 ms	Yes
34 to 4 $\mu$ N	190 ms	FEE-106	50 ms	Yes
70 to 100 $\mu$ N	190 ms	FEE-106	50 ms	Yes
100 to 70 $\mu$ N	190 ms	FEE-106	50 ms	Yes

(\*) including 20ms to take into consideration delay time of the thrust command processing inside the FPGA (worst case time).

**Table 3.1: Transient response time summary.**

NOTE 1: Transients from 0 to 150  $\mu$ N and from 150 to 0  $\mu$ N were performed with HV probe for measurement of the emitter voltage. Due to the effect of the probe as additional load, these measurements are provided for reference only.

NOTE 2: Requirement FEE-864 refers to thrust overshoot.

For the GG application, response time for the step 10 to 150  $\mu$ N (TBC) will be improved, according to sect. 6.2.

### 3.5.5 Arcing

Analysis of spark rate was conducted on the basis of Endurance Test #2.

In the following table and diagram, spark rate is analyzed with respect to thrust level, in the range of interest.

Thrust range	Number of sparks recorded	Minimum time between sparks (s)	Maximum time between sparks (s)	Mean time between sparks (s)	Average spark rate (sparks/hour)
0-10	830	2	12664	273	13
10-20	465	2	25794	621	6
20-30	730	2	16880	394	9
30-40	81	3	13966	562	6
40-50	594	2	7214	372	10
50-60	524	3	28800	577	6
60-70	80	2	6609	524	7
70-80	12032	2	42685	483	7
90-100	6789	2	23538	374	10
Overall	26099	2	42685	423	9

**Table 3.2: Recorded spark rate vs. thrust level.**

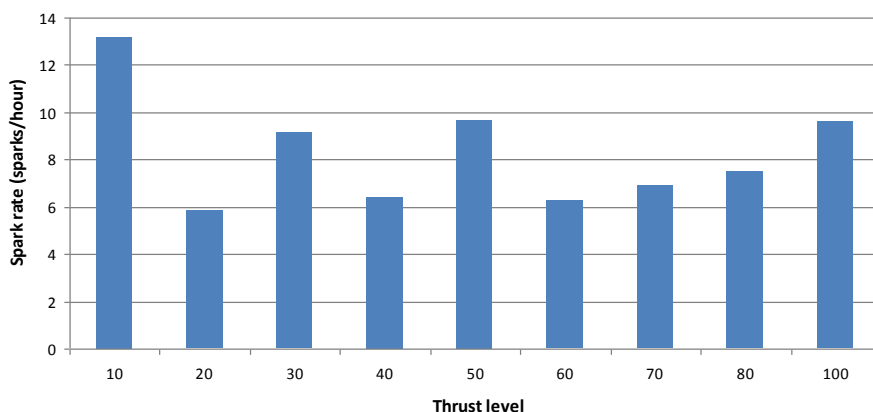


Figure 3.18: Recorded spark rate vs. thrust level.

The following table and diagram show the distribution of intervals between sparks (grouped for minute and regardless of thrust level), in the range 0 to 1 hour.

From (sec)	To (sec)	Number of sparks	Fraction	From (sec)	To (sec)	Number of sparks	Fraction
1	60	5867	22.48%	1800	1860	55	0.21%
60	120	3733	14.30%	1860	1920	39	0.15%
120	180	2876	11.02%	1920	1980	46	0.18%
180	240	2214	8.48%	1980	2040	47	0.18%
240	300	1839	7.05%	2040	2100	51	0.20%
300	360	1494	5.72%	2100	2160	32	0.12%
360	420	1087	4.16%	2160	2220	33	0.13%
420	480	897	3.44%	2220	2280	33	0.13%
480	540	770	2.95%	2280	2340	28	0.11%
540	600	646	2.48%	2340	2400	26	0.10%
600	660	506	1.94%	2400	2460	16	0.06%
660	720	432	1.66%	2460	2520	20	0.08%
720	780	363	1.39%	2520	2580	22	0.08%
780	840	317	1.21%	2580	2640	23	0.09%
840	900	303	1.16%	2640	2700	19	0.07%
900	960	228	0.87%	2700	2760	23	0.09%
960	1020	185	0.71%	2760	2820	18	0.07%
1020	1080	219	0.84%	2820	2880	12	0.05%
1080	1140	159	0.61%	2880	2940	7	0.03%
1140	1200	126	0.48%	2940	3000	14	0.05%
1200	1260	125	0.48%	3000	3060	10	0.04%
1260	1320	107	0.41%	3060	3120	18	0.07%
1320	1380	122	0.47%	3120	3180	17	0.07%
1380	1440	87	0.33%	3180	3240	16	0.06%
1440	1500	75	0.29%	3240	3300	14	0.05%
1500	1560	76	0.29%	3300	3360	10	0.04%
1560	1620	69	0.26%	3360	3420	13	0.05%
1620	1680	55	0.21%	3420	3480	14	0.05%
1680	1740	70	0.27%	3480	3540	16	0.06%
1740	1800	72	0.28%	3540	3600	9	0.03%

Table 3.3: Distribution of sparks vs. interval between sparks (in minutes).

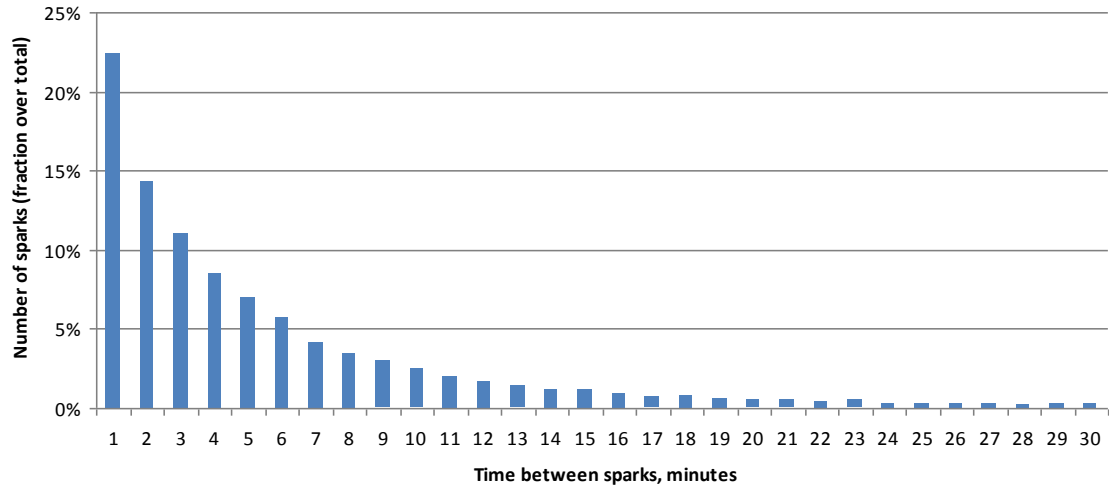


Figure 3.19: Distribution of sparks vs. interval between sparks (in minutes).

Finally, the following table and diagram show the evolution of spark rate with time (cycles of Endurance Test).

	Number of sparks recorded	T-on time (hours)	Average spark rate (sparks/hour)
Cycle 1	1147	167.28	6.86
Cycle 2	603	164.77	3.66
Cycle 3	701	168.88	4.15
Cycle 4	1155	171.04	6.75
Cycle 5	444	166.79	2.66
Cycle 6	293	166.01	1.76
Cycle 7	440	167.96	2.62
Cycle 8	1402	167.7	8.36
Cycle 9	2233	167.69	13.32
Cycle 10	3106	189.21	16.42
Cycle 11	2871	171.52	16.74
Cycle 12	2755	166.61	16.54
Cycle 13	2087	142.51	14.64
Cycle 14	1204	167.7	7.18
Cycle 15	1030	166.8	6.18
Cycle 16	919	104.2	8.83

Table 3.4: Time evolution of spark rate.

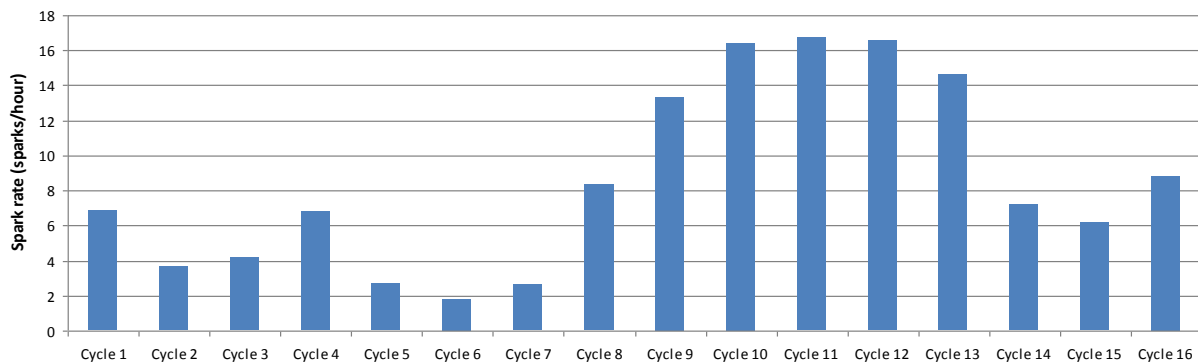


Figure 3.20: Time evolution of spark rate.

### Conclusions

The performed analysis shows that:

- spark rate is not dependent on thrust level;
- sparks tend to be grouped: short time intervals between sparks are more frequent than long ones;
- spark rate is not time dependent: Figure 3.20 shows that, after a phase of relatively high sparking rate, the rate returns to values comparable with the beginning of the test.

Analysis of temperature correlation or chamber pressure correlation was not performed. It is however believed that the spark rate is strongly influenced by the vacuum facility environment (pressure and contamination), and that in-flight performance will be much better in terms of arcing frequency.

Spark “energy” evaluation (analysis of spark-induced disturbance on control system) is addressed by [RD 6].

#### 3.5.6 Total impulse and specific impulse

At present, about 1000 Ns were demonstrated by Endurance Test No. 2 (3228 hours of firing time), when neglecting any limit on accelerator current or, alternatively, about 500 Ns were achieved before the current limit of 800  $\mu$ A was reached.

Actual total impulse capability will be verified by the Life Test, where the capability to keep the accelerator current low enough will also be verified.

Average in-flight specific impulse has been evaluated for Lisa Pathfinder based on the results of following three tests:

- neutral flow measurement test, performed at Onera Palaiseau premises;
- Direct Thrust Measurement (DTM#2) test, performed at TAS-I Turin premises;
- Endurance Tests No. 1 and No. 2, performed at Alta premises.

For the Lisa Pathfinder specific constraints (e.g. typical thrust profile, total impulse EOL equal to 2045 Ns), the following assessment was made:

- the average Isp at EOL is about 3200 s;
- the residual propellant mass at EOL is about 25 g (out of 90 g).

#### 3.5.7 Thruster beam divergence

Figure 3.21 shows the summary of beam divergence angles (including 99% of the beam) recorded during TAPT#2 and following Endurance Test No. 2. The plot shows how the beam divergence increases at very low thrust values (higher average values at 150  $\mu$ N are due to the lower numerosness of the data sample).

Since the beam divergence information is applicable to contamination effects, the average value (and not maximum ones) is of concern. The plot above shows that the Lisa PF requirement is met by the average beam divergence on both planes of measurement, down to a thrust value in the order of 10  $\mu$ N. At lower thrust values, the average divergence angle is higher than specification. However, also the ion current is reducing for lower thrust, which means contamination is still very low.

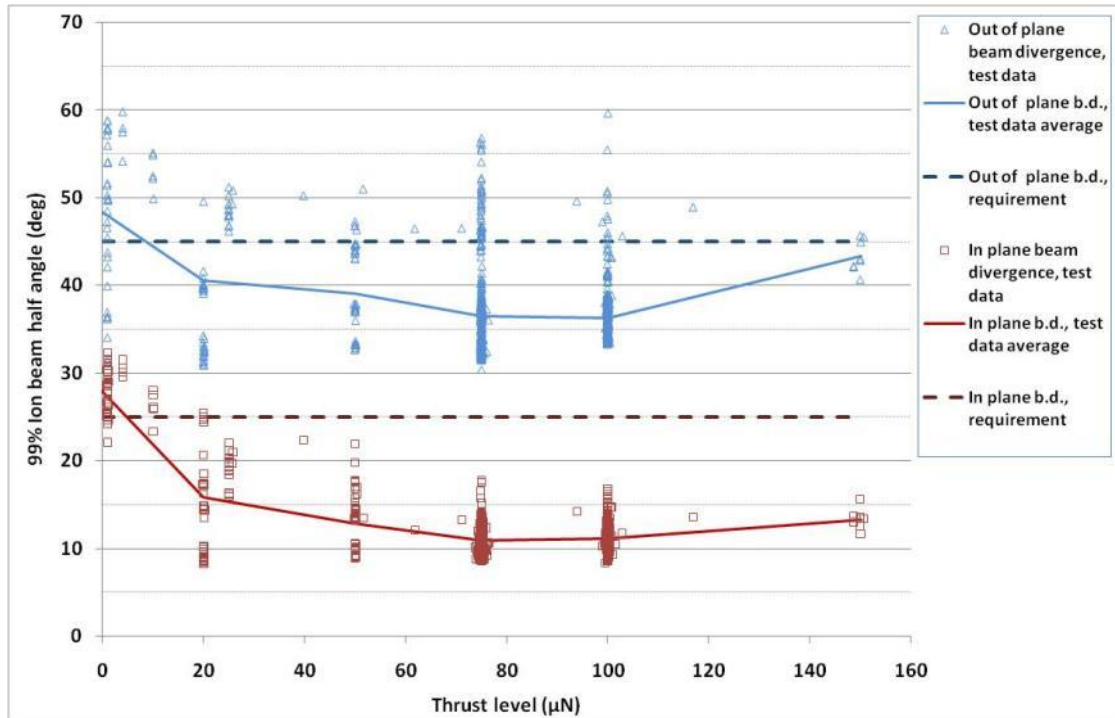


Figure 3.21: Beam divergence (99% of beam), from TAPT#2 and Endurance Test #2, vs. thrust level.

### 3.5.8 Thrust vector errors

The error between the nominal thrust vector and the instantaneous thrust direction is made up of the following terms:

- short and long term fluctuations of the ion beam;
- thrust vector uncertainty due to internal thruster mounting and thermal deformations;
- machining tolerances on the thruster interface and the cluster structure;
- thermal effects on the cluster.

The terms above are assumed linearly cumulating and all acting in the same plane (worst case assumption for angles).

In reverse order:

- during nominal operation the cluster thermal environment is kept stable by the thrusters thermal control. Under these conditions, misalignment of electrodes can be neglected;
- machining tolerances on the thruster interface and the cluster structure affecting alignment are:
  - interface washers thickness ( $\pm 0.05$  mm tolerance);
  - thruster I/F flange parallelism ( $\pm 0.05$  mm tolerance);
 these contribute to a maximum misalignment of 0.5 deg.
- Internal thruster tolerances and deformations affect the beam direction if the accelerator electrode is shifted with respect to its nominal position on the emitter symmetry plane. With machining tolerances and design, it can be ensured misalignment is not exceeding 0.05 mm, which implies a beam deflection lower than 1.2 deg (at maximum thrust, i.e. 150 μN).

The above terms add up (in the worst case) to a value of 1.7 deg (@ 150 μN) for geometrical effects.



The additional error that can be measured during tests is therefore due to variation of thrust vector as a function of thrust level and time.

The following plot shows a summary of thrust vector angle measurements collected during TAPT#2 and following Endurance Test #2. The measured thrust angle is plotted as a function of thrust level, showing the deviation from nominal direction is lower for increasing thrust levels. The test results include already geometrical errors (due to internal thruster misalignment and misalignment of the thruster w.r.t. the beam probes system, that are evidenced by the mean 1.7 deg thrust angle recorded at 150  $\mu$ N. The figure shows the average thrust angle increases largely in the low thrust region.

The figure also provides a proposed “Thrust angle error budget” line. Such line was obtained by finding one hyperbola that envelops all (100%) data points, with maxima multiplied by a 10% margin factor.

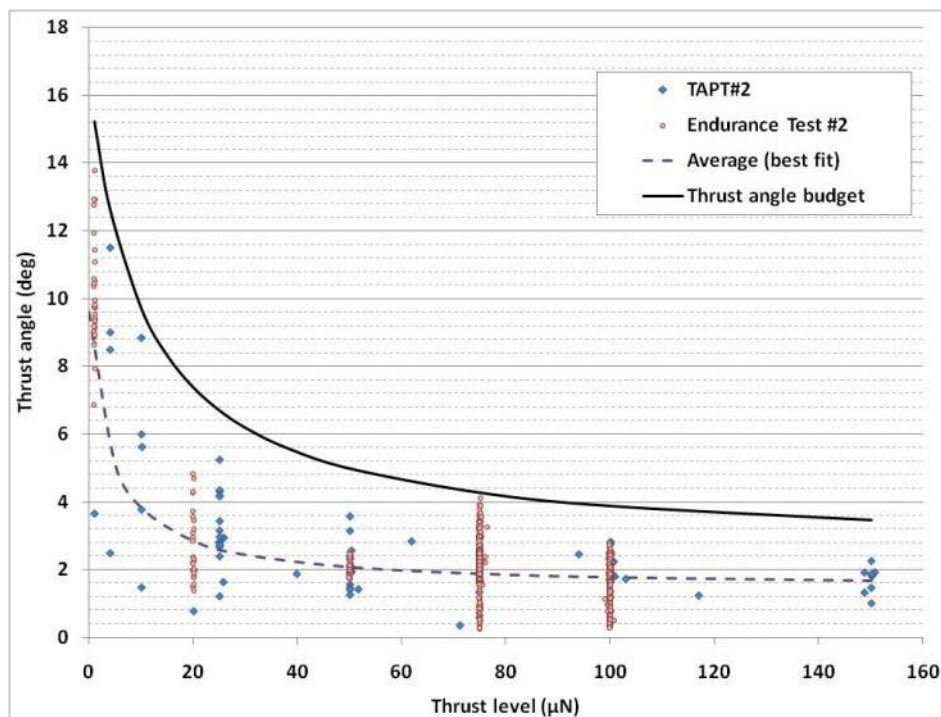


**Figure 3.22: Thrust angle vs. thrust level measured during TAPT#2 and Endurance Test #2, and corresponding thrust angle budget.**

If one considers the requirement in terms of lateral disturbance, the thrust level shall be multiplied by the sine of the thrust vector angle. Figure 3.23 shows that, even if the angular deviation is higher, the lower thrust levels are still less critical than the higher ones w.r.t. lateral force.

Finally, Figure 3.24 shows the components of the lateral force vector, in the plane orthogonal to thrust direction, which provides an indication of how the thrust vector errors translate into lateral disturbance.



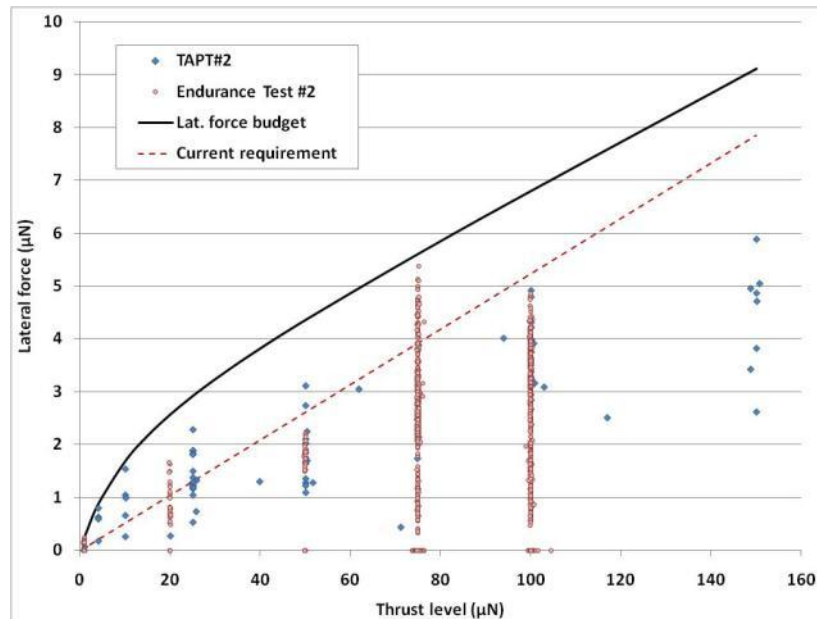


Figure 3.23: Lateral force vs. thrust level measured during TAPT#2 and Endurance Test #2, and corresponding lateral force budget.

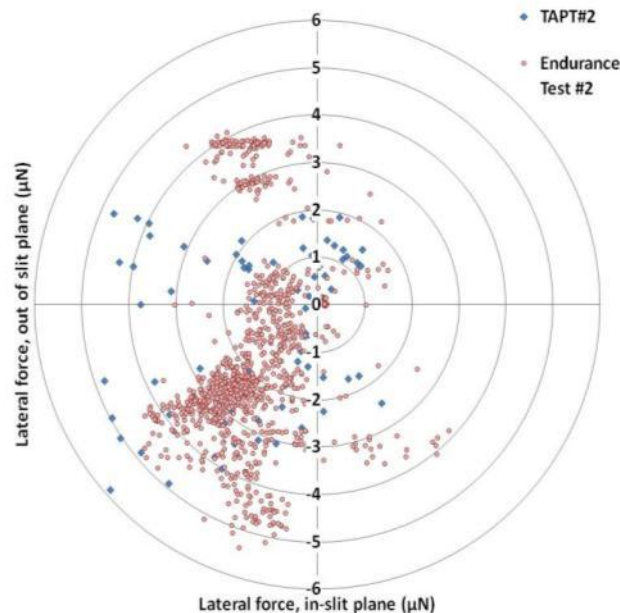


Figure 3.24: Lateral force direction measured during TAPT#2 and Endurance Test #2.

### 3.5.9 Command frequency

In current applications the thrust command can be processed with a frequency up to 10 Hz (actual rate is 10 Hz on LPF and 4 Hz on Microscope).

The electronic units were designed for such requirement, and for the thrust response times described in sect. 3.5.4.

### 3.6 Other relevant test results and verification achievements

In addition to all the performance tests performed and referenced above (thruster performance was characterized during the Lisa Pathfinder development phase by testing more than 15 thrusters, at various levels of representativeness), testing was performed also at cluster and subsystem level. In particular:

- a thruster cluster Development Models (cluster structure with one thruster and 3 mass dummies) underwent three mechanical testing campaigns (two sine and random vibration tests and one acoustic testing at S/C level), verifying robustness of thruster design to mechanical testing and allowing improvement of FEM models;
- a full thruster cluster (FCA) with four thrusters underwent Thermal Balance testing in ESTEC, verifying robustness of cluster design to thermal stresses and allowing improvement of thermal models;
- a complete subsystem section (one thruster, one PCU and one neutralizer) were tested in ESTEC EP laboratory to verify the neutralization concept. The subsystem was kept electrically floating in the vacuum chamber, and it was verified that the neutralizer effectively regulates the subsystem potential, emitting a neutralization current which is exactly compensating the ionic one.

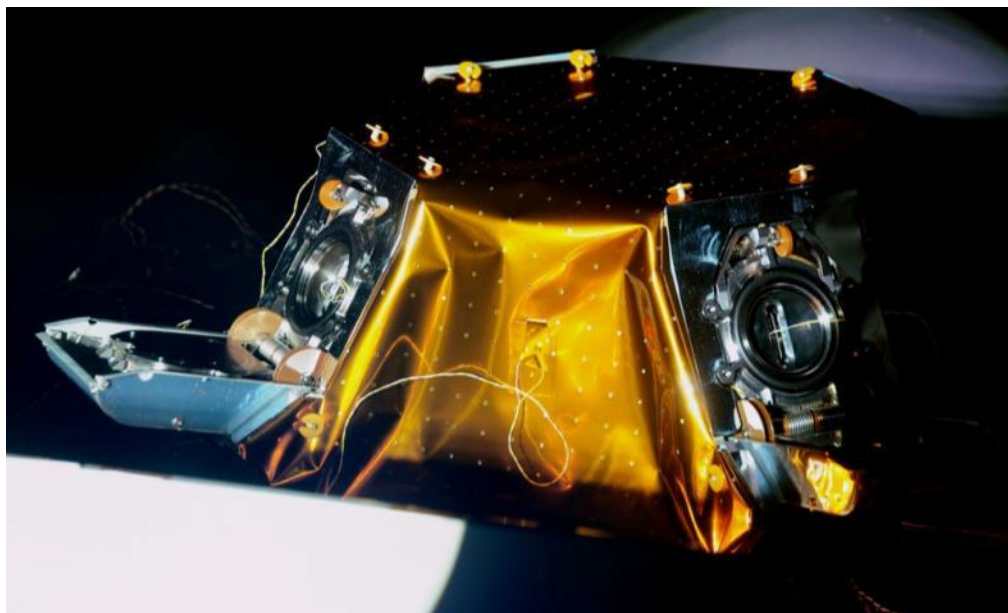


**Figure 3.25: FCA during thermal balance test.**

## 4 Thruster requirements for GG application

The following table provides the status of compliance of the FEEP technology with respect to GG technical requirements. Requirements implying a delta-design and/or a delta-verification are highlighted. No non-compliance is expected and criticality level of requirements yet to be verified is low. The only critical requirement that was identified during the phase A2 study is the centrifugal acceleration. However, the reduced spin rate (from 2 Hz to 1 Hz) and the consequent reduction in acceleration (from 17.6 to 4.4 g's) makes the required modifications much easier. A design solution has been already identified and is described in sect. 6.1.

No	Parameter	Unit	Value	SoC (C/NC)	Justification	Verification status
1	Maximum thrust	$\mu\text{N}$	$\geq 150$	C	$> 200 \mu\text{N}$ can be provided by current design	Verified by DTM.
2	Thruster response time	ms	40	C	Can be achieved through minor changes in PCU design (see sect. 6.2).	To be verified by testing at PCU EBB level.
3	Resolution (quantization)	$\mu\text{N}$	$< 24$	C	$0.1 \mu\text{N}$ resolution verified with current design	Verified by TAPT#2 and DTM tests.
4	Max noise	$\mu\text{N}/\sqrt{\text{Hz}}$	18 @ 1Hz	C	$< 0.1 \mu\text{N}/\sqrt{\text{Hz}}$ recorded in range $10^{-3}$ to 5 Hz.	Verified by TAPT#2 and DTM tests.
5	Scale factor error	%	12 peak	C	$< 8\%$ measured	Verified by DTM.
6	Update com rate	Hz	10	C	Same as current LPF design.	Verified at PCU level (qualification)
7	Total impulse	Ns	4500	C	Propellant tank will be designed for enough cesium capability. No electrodes degradation occurs during life test. Internal dissipation at EOL to be assessed.	To be verified by review of design (upgraded tank) and analysis (extrapolation of Lisa Pathfinder 1100 Ns life test results).
8	Minimum thrust	$\mu\text{N}$	$\leq 10$	C	Minimum thrust capability is $0.1 \mu\text{N}$	Verified by TAPT#2 and DTM tests.
9	Vector stability	rad	0.17 @ 60 $\mu\text{N}$	C	Thrust vector error lower than 8 deg in the range 10 to $150 \mu\text{N}$	Verified by ET#2.
10	Specific impulse	s	$> 60$	C	Isp $> 3000$ s EOL expected.	Verified by ET#2, LIF test, DTM.
11	Centrifugal acceleration	$\text{g's}$ ( $\text{m/s}^2$ )	$< 4.4$ (43.2)	C	Propellant tank and TA layout will be designed to comply with 4.4 g with margin (see sect. 6.1).	To be verified by testing at thruster EM level (max sustainable hydrostatic pressure).
12	Number of thrusters per cluster		8 or 12	C	See section 5.	Verified by review of design.

**Table 4.1: Matrix of compliance to technical requirements.**

## 5 Propulsion system architecture and design

### 5.1 Subsystem architecture

The proposed Micro-thrusters system architecture for GG is based on the following diagram:

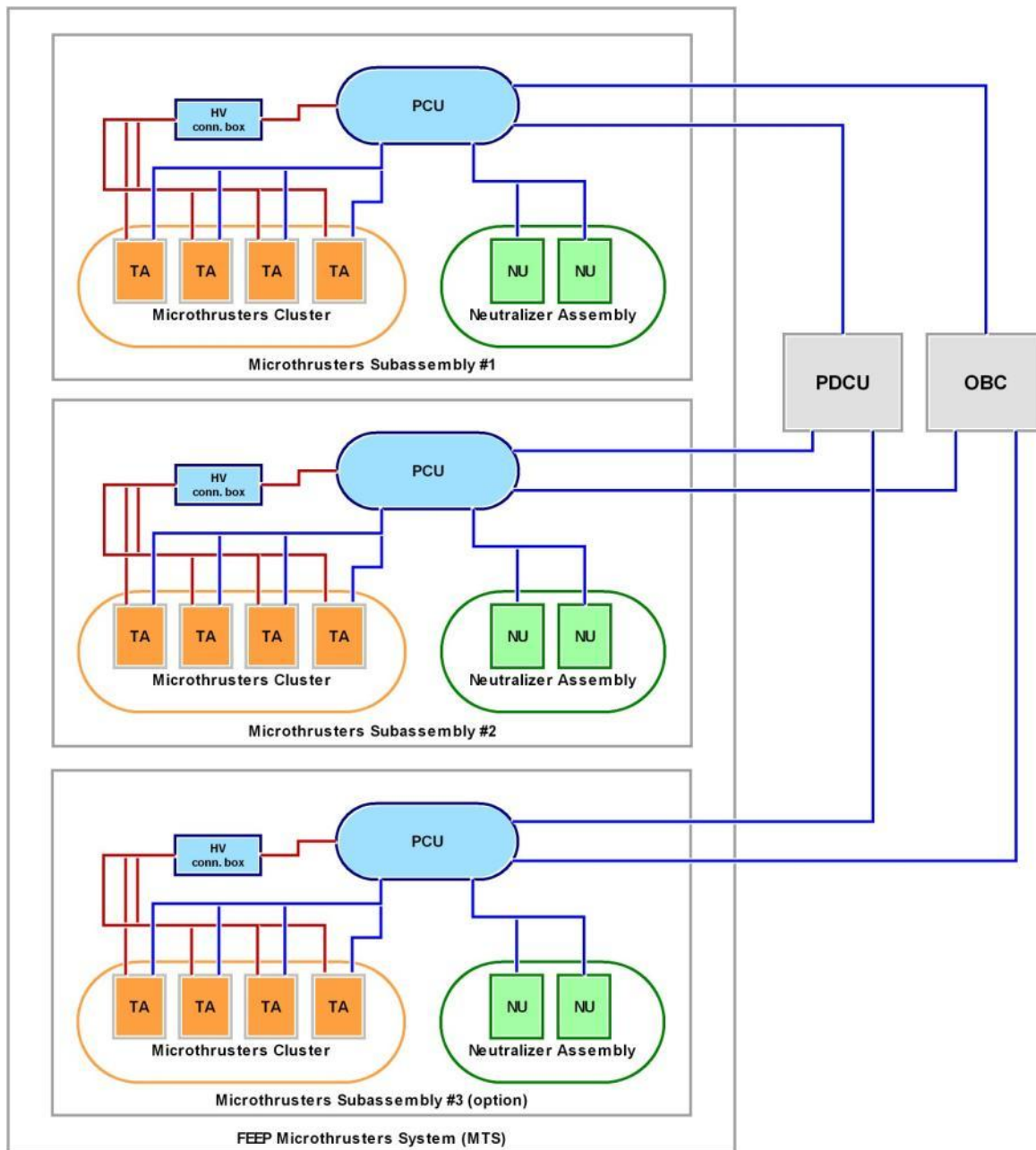


Figure 5.1: FEEP Microthrusters System architecture.

The system is based on 2 or 3 (depending on selected option) independent Microthrusters Subassemblies (MTSA), each composed of the following elements:

- one PCU, capable to control 4 thrusters and one neutralizer unit at the same time (plus one NU in cold redundancy);
- one Micro-Thrusters Cluster (MTC), made of four identical thrusters, aligned according to required thrust directions;
- one Neutralizer Assembly (NA), comprising two Neutralizer Units, operated in cold redundancy;
- one HV connection box, for mating of the PCU and Thrusters HV lines.

Each PCU is connected to the main bus (PCDU) by two power lines (one main and one redundant), and to the On-Board Computer by two MIL-STD-1553 TC/TM interfaces (one main and one redundant). It is also connected to the four thrusters of the MTC by individual LV connection lines (one 15-pin connector per thruster) and by brazed and potted HV cables (one cable per electrode, i.e. 8 lines per cluster). Finally, PCU is connected to the neutralizers by individual LV connection lines (one 9-pin connector per neutralizer unit).

Additional monitoring and power supply lines between units and the system (e.g. survival heaters power supplies from PDCU to MTC) shall be agreed with the Prime Contractor.

## 5.2 Product tree

The product tree for the FEEP MTS is shown in the following picture:

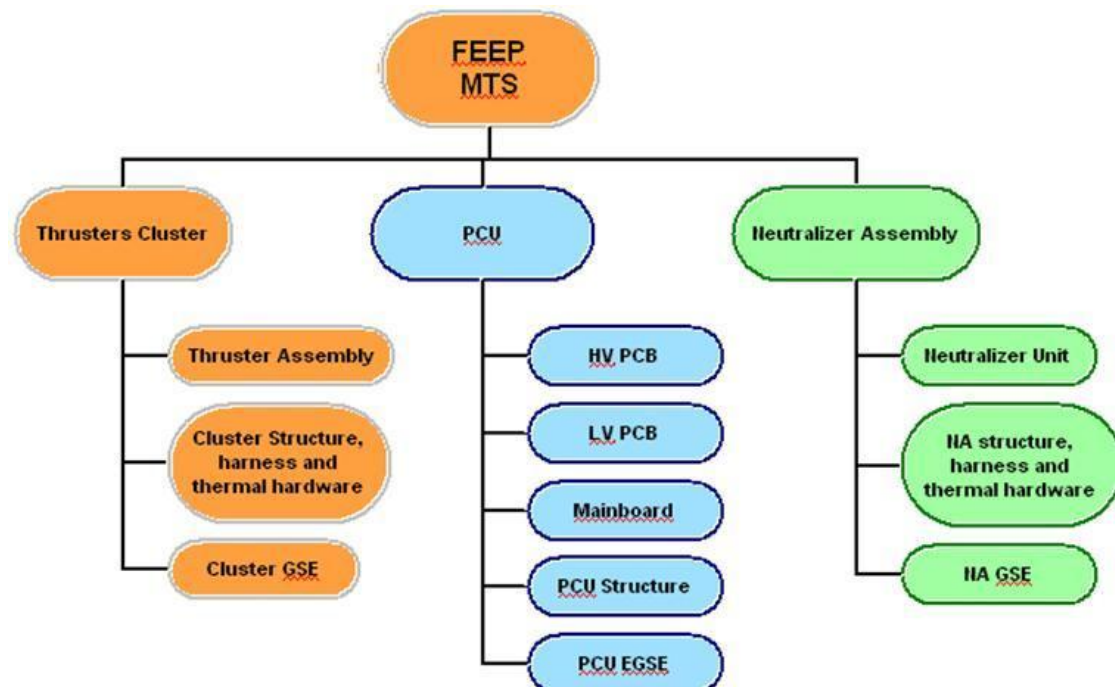


Figure 5.2: High level Product Tree of the FEEP Micro-Thrusters System for GG.



### 5.3 Micro-Thrusters Cluster (MTC) design

The MTC layout is shown in the following pictures. Thrusters are mounted in order to verify the following constraints:

- thrust directions are according to the specified angles;
- propellant reservoirs are aligned with a plane parallel to spin axis, in order to minimize hydrostatic pressure.

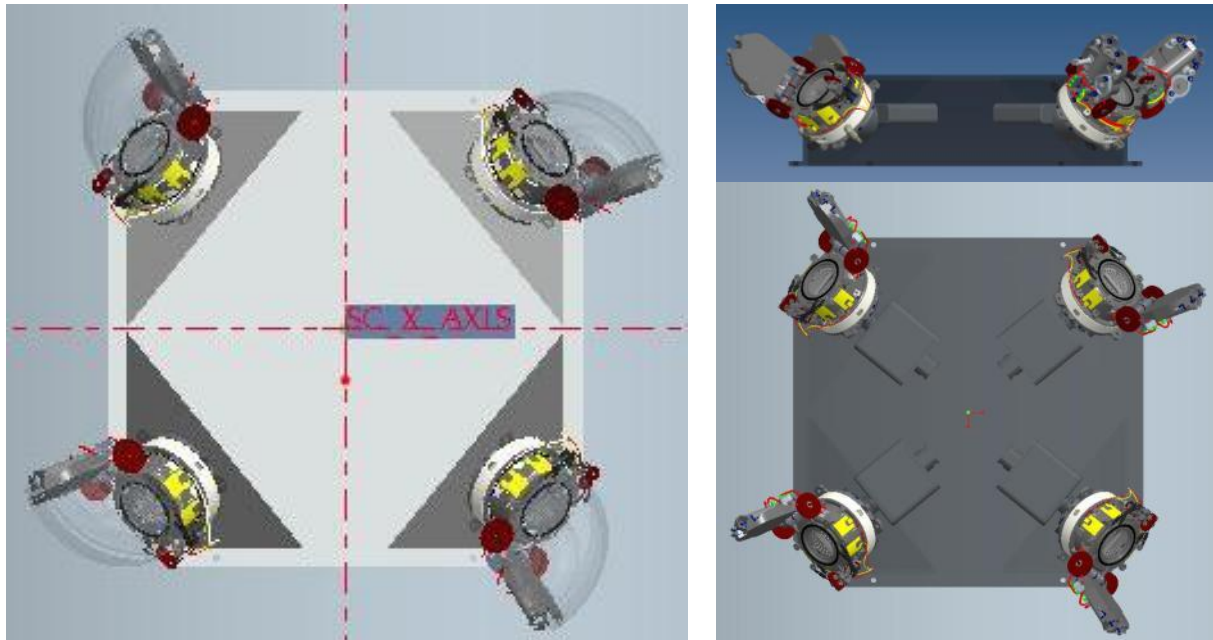


Figure 5.3: MTC layout (left). Position of propellant reservoirs highlighted (right).

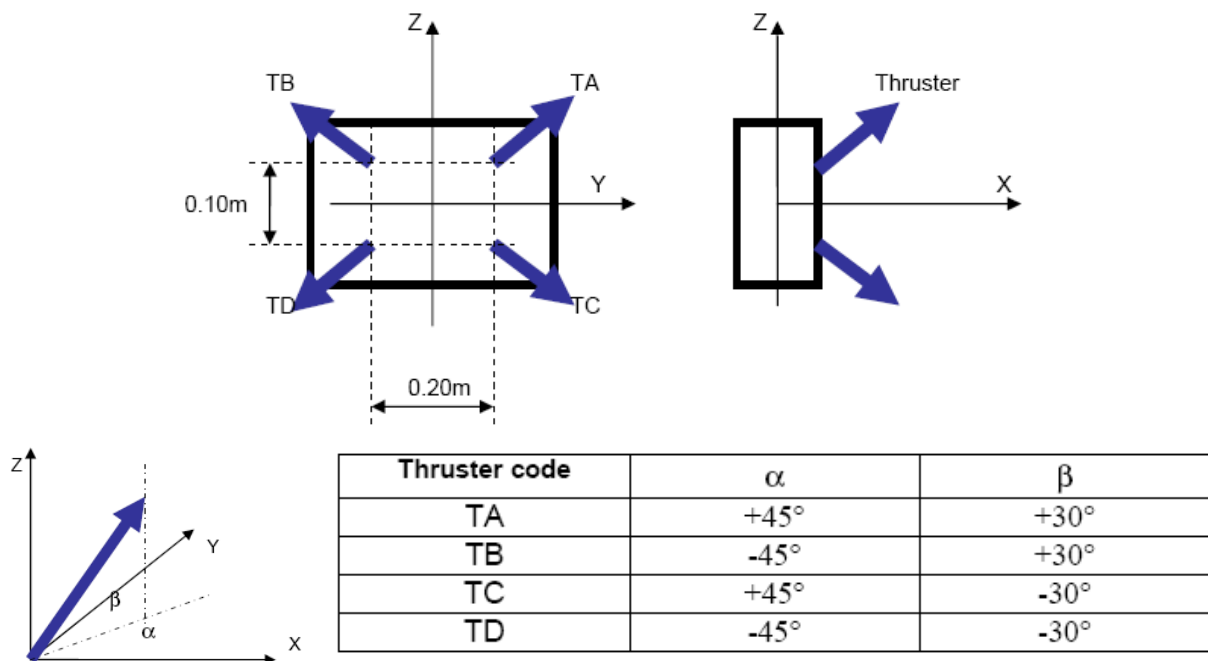
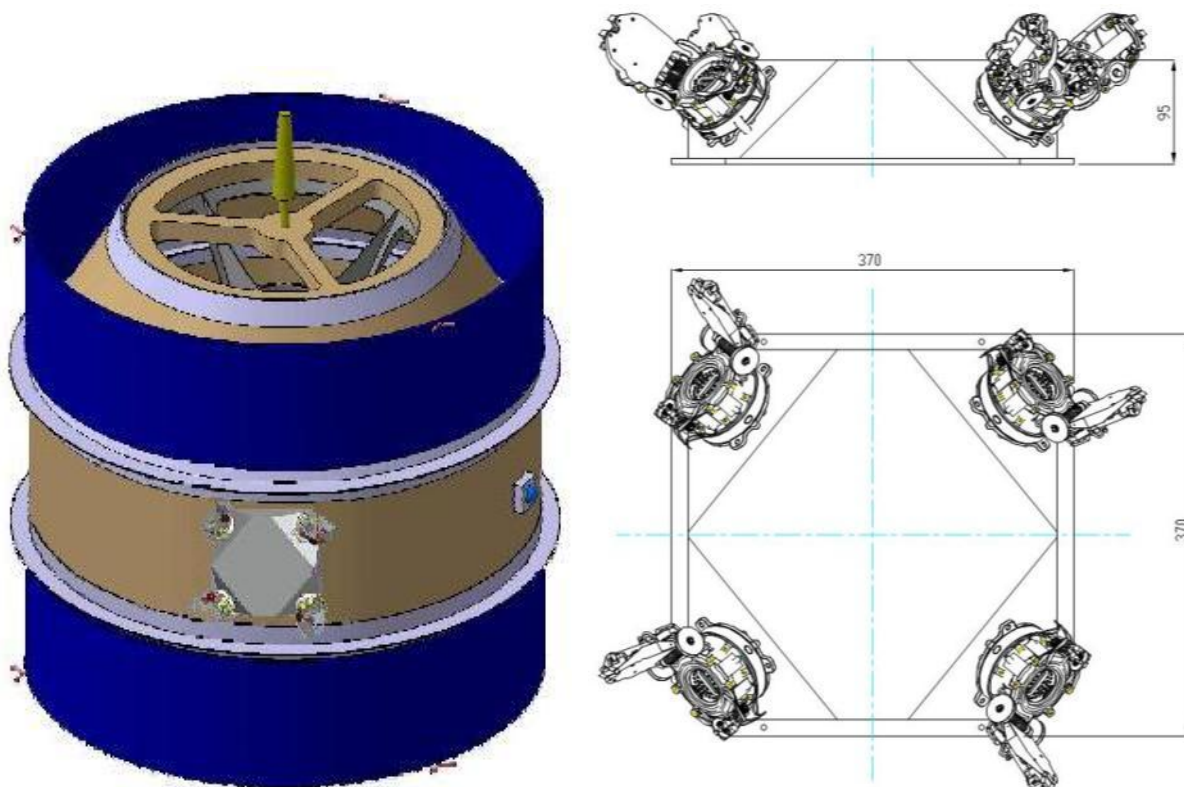
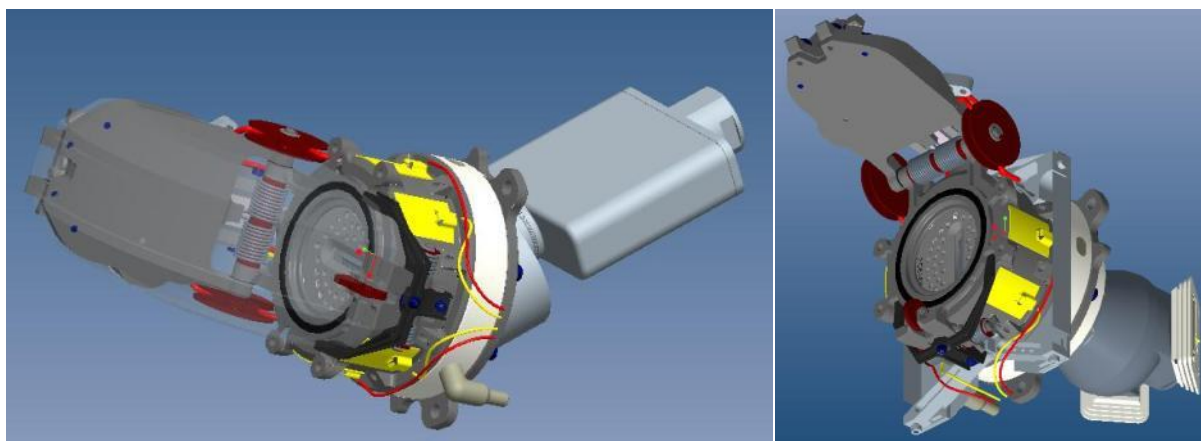


Figure 5.4: Thrust direction angles.



**Figure 5.5: MTC mounted on GG spacecraft (left) and thruster cluster structure gross dimensions (right).**

### 5.3.1 Thruster Assembly description



**Figure 5.6: Thruster assembly for GG (left) and for Lisa Pathfinder (right).**

Thruster is based on the same design of the Lisa Pathfinder (LPF) unit, with the only exception of the tank, which is designed on purpose for the mission. Existing LPF tank is designed on capillarity, to operate in microgravity environment. In the case of GG, the tank shall be designed to operate in enhanced gravity environment, i.e. with an hydrostatic pressure deriving from centrifugal forces due to spin. Preliminary design of tank is described in sect. 6.1.

## 5.4 PCU design

The Power Control Unit (PCU) proposed for Galileo Galilei (GG) mission is based on the existing equipment already developed in the frame of the Lisa Pathfinder mission, and described in sect. 3.3.

The required design upgrades to match GG step response requirement are described in sect. 6.2.

## 5.5 Neutralizer Assembly description

The Neutralizer Assembly shall be provided as CFI by Thales Alenia Space. The existing Lisa Pathfinder design, described in section 3.4, fulfils the requirements of GG, as of current specifications. An equipment technology readiness review will be performed to verify if NA qualification covers all the GG requirements (including mechanical and thermal environments).



## 6 Design modifications to meet GG requirements

According to compliance matrix in sect. 4, there are just two requirements prompting for a design modification:

- the centrifugal acceleration value implies a (major) modification to propellant tank design, in order to reduce the hydrostatic pressure at emitter slit level, avoiding the risk of propellant spillage;
- the required step response time (and the amplitude of the thrust variation step) implies a minor modification to PCU design, to improve this performance parameters.

These changes are described in the following sections.

### 6.1 Thruster Assembly

#### 6.1.1 Required design change

The maximum theoretical pressure (considering real geometry and worst case cesium surface tension) that the liquid meniscus on the tip of the thruster can sustain is in the order of 10 to 20 kPa (i.e. 0.1 to 0.2 bar, or 100 to 200 mbar). Imperfections in the emitter geometry and boundary effects make this limit somewhat lower. Conservatively, Alta assumes a factor of safety equal to 5 on the minimum pressure value, i.e. **2000 Pa** (20 mbar) are assumed as the (preliminary) design value for maximum hydrostatic pressure. As detailed in sect. 6.1.3 below, this design parameter is subject to revision after a dedicated engineering test.

In the specified acceleration environment, the maximum hydrostatic head of propellant (maximum distance between emitter tip and propellant level along the S/C radial direction, i.e. maximum delta-distance from spin axis) is:

$$\max \Delta h = \frac{\max p}{\rho_{CS} \cdot a_c} = \frac{2000}{1844 \cdot 4.4 \cdot 9.81} \text{ m} \cong 0.025 \text{ m} = 2.5 \text{ cm} \quad (6-1)$$

This implies that:

- the tank can have a maximum width, along the radial direction, of 2.5 cm;
- the tank shall lie flat at the same level of the emitter, with its inner surface (“top” in the local gravity reference) not closer than 2.5 cm to the spin axis than the emitter tip, and its outer surface (“bottom” in the local gravity reference) not further from the spin axis than the emitter tip (to avoid residuals in the tank that cannot overcome the centrifugal acceleration to reach the emitter).

The following pictures show a preliminary schematic layout of the tank and of how the Thruster Assembly would look like.

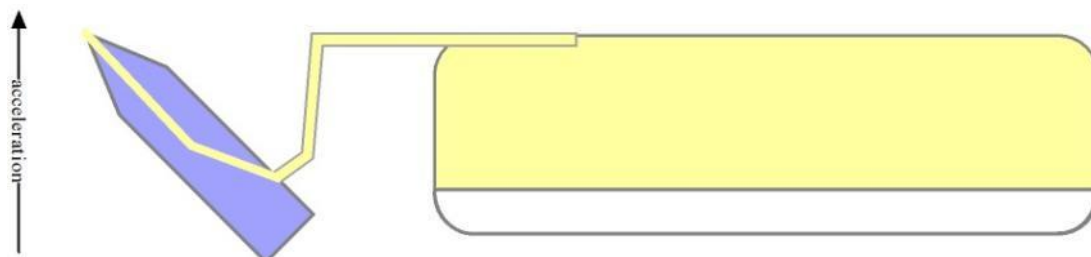
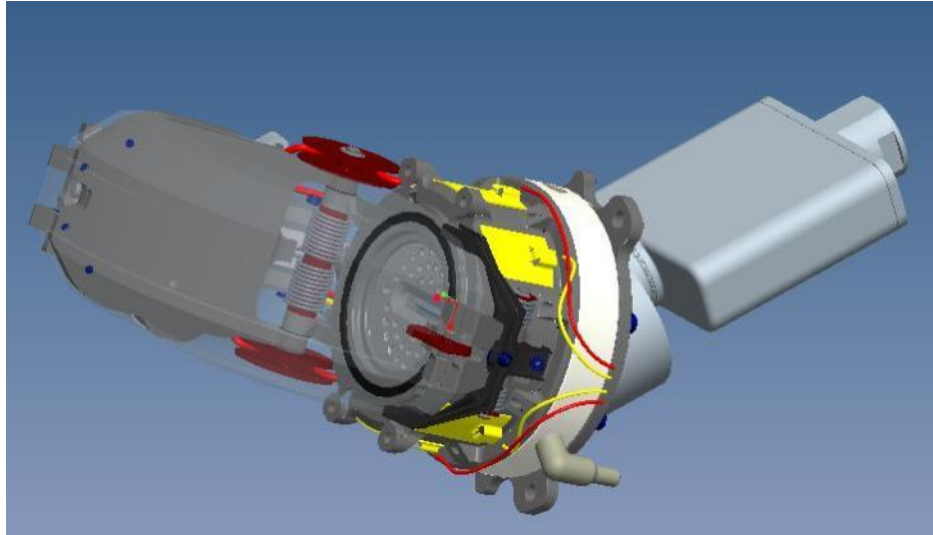


Figure 6.1: Tank preliminary layout (scheme).



**Figure 6.2: Preliminary TA layout.**

### 6.1.2 Advantages/disadvantages

The major disadvantage of the revised tank design is that the tank will need to be re-qualified, and the existing design cannot be entirely used “as is”.

On the other hand, besides solving the issue of the high local acceleration without imposing thrusters relocation (moving thrusters closer to spin axis would reduce acceleration level), the new tank would have some beneficial features with respect to the existing one:

- considering there is no need for the tank to operate in capillary mode, there is no need for a Propellant Management Device (PMD). This means the tank design can be simpler than current one, and there is no need to have a PMD specialist in charge of Tank design and manufacturing (on Lisa Pathfinder tank is procured by Astrium SAS – Toulouse). The tank can then be designed, manufactured and qualified by Alta, making the technology a 100% Italian one;
- on Lisa PF capillarity also imposes the tank being made of Inconel (for cesium wetting reasons). On GG there would be no need to have a maximum guaranteed wetting angle, and titanium alloy can perfectly do the job. This means the tank can be lighter than current one (although the amount of propellant would be larger).

### 6.1.3 Risk mitigation

Since both the Lisa Pathfinder and the Microscope mission operate in microgravity, test efforts so far were directed in showing the thruster can operate with a minimum, or even negative hydrostatic head (to this aim, thruster is usually tilted upwards during the tests). In those tests where hydrostatic pressure was present (propellant level was higher than emitter one), Alta demonstrated that the thruster can sustain without troubles an hydrostatic pressure in excess of about 200 Pa.

Since the assumed design limit is 10 times higher than this, the suitability of such critical design parameter has to be assessed very early in the project. For this reason, Alta will perform a dedicated test (with a suitable thruster Engineering Model and ad-hoc test set-up) to measure the limit sustainable hydrostatic pressure and, therefore, the most suitable design limit and the related design margin.

## 6.2 PCU

### 6.2.1 Required design change

Limited modifications are required to meet the GG requirement with respect to PCU LISA Pathfinder design. These changes aim at meeting the thrust response time requirement, i.e. 40 ms to achieve 90% of commanded thrust step, for a step from minimum thrust (10  $\mu$ N) to maximum thrust (150  $\mu$ N, tbc), and back (max to min).

The following modifications are proposed:

- Increasing of the thrust control loop operating frequency (e.g. from 50 to 100 Hz) in order to reduce the delay from the thrust command and the loop itself (which are asynchronous). FPGA will be updated accordingly.
- Increasing of the HV power supply capability and filtering stage to sustain the energy of the HV section to support the required rise time. Power Board will be updated accordingly.

### 6.2.2 Advantages/disadvantages

The advantage of improving the step response time would carry along minor disadvantages (e.g. increase in noise level) that are not affecting the overall compliance status due to the large margins available (e.g. a factor 180 on thrust noise).

### 6.2.3 Risk mitigation

To mitigate the programmatic risks, it is foreseen to anticipate the design modifications to phase B, and perform a test on existing PCU Elegant Breadboard (EBB), suitably modified, to verify the changes are effective and the other performance parameters are not significantly affected (see Development Plan in section 9).

## 7 Interfaces

### 7.1 Electrical interfaces

The electrical interfaces for the FEEP subsystem are summarized in the following:

- for each PCU, two power interfaces, one main and one redundant (cold redundancy). 28 V regulated power bus is assumed as baseline;
- for each PCU, two command/telemetry interfaces, one main and one redundant (cold redundancy). MIL-STD-1553 is assumed as baseline;
- survival heaters power lines (regulated 28 V line), TBC (depending on thermal analysis and planned safe mode / OFF mode durations);
- external TRP temperature telemetry (recommended but not mandatory).

Connectors type and pin functions will be specified at a later stage of the programme.

Grounding will be allowed via dedicated bonding studs on all units (PCU, MTC, NA).

### 7.2 Mechanical interfaces

The three units of the Micro-Thrusters System will interface to the spacecraft according to the following (preliminary) mechanical interfaces:

Unit	Units no.	Position	No. of mounting feet (per unit)	Type of fitting (all TBC)
MTC	2 or 3	External panel, external side	8 (TBC)	M5 screw, socket head
PCU	2 or 3	External panel, internal side	6	M5 screw, socket head
NA	2 or 3	External panel, external side	4	M5 screw, socket head

**Table 7.1: MTS mechanical interfaces.**

Dimensions and footprint (preliminary for MTC) are provided in Appendix A.

### 7.3 Thermal interfaces

The Micro-Thrusters Cluster (MTC) will be as far as possible thermally decoupled from the spacecraft, embedding thermal washers to minimize conduction, internal heaters to control temperature, and thermal blankets (MLI) to reduce power dispersion by radiation to space. Thermal Conductance (GL) between MTC and S/C will be in the order of 0.1 W/K (TBC).

Information on Neutralizer Assembly thermal interfaces can be found in [RD 7].

The PCU will need thermal coupling with the S/C panel, to reject internally generated heat by conduction to the S/C panel. Information of heat fluxes in the various operative conditions can be obtained using the delivered power consumption model (Excel spreadsheet).

## 8 Operational constraints and limitations

### 8.1 EMC/ESD

The FEPP subsystems are designed for the very demanding EMC requirements of drag-free missions such as Lisa Pathfinder and Microscope. In particular, FEPP design features:

- almost no use of magnetic materials;
- good design practices in EMC control;
- very low current in generated ion beam (usually less than 1.5 mA).

There are no valves, solenoids or any other type of electro-magnetic actuators among the FEPP system components. All current-carrying cables are twisted and shielded as far as possible. All High voltage cables and parts are shielded by at least one metallic braid or structural wall. Signal lines are double shielded where applicable. All heaters are made with non-inductive patterns.

In terms of DC magnetic moment, the following requirements are specified, at unit level, for the Lisa Pathfinder programme:

- $< 100 \text{ mAm}^2$  for the thruster cluster (with 4 active thrusters);
- $< 10 \text{ mAm}^2$  for the Neutralizer Assembly (with 1 active neutralizer unit);
- $< 300 \text{ mAm}^2$  for PCU.

DC magnetic moment measurement, as well as full EMC testing (CE/CS, RE/RS and DC/AC magnetic field measurements) will be performed in the frame of the Lisa PF units and subsystem qualification. At present, it is expected that the units will perform as specified.

Some EMI concern, peculiar to ion thrusters, is related to the presence of sparks (see also sect. 3.5.5 and [RD 6]).

However:

- sparks are internal to the thruster, they occur between the emitter and the accelerator;
- spark phenomena are very fast, they last for few (2 to 10)  $\mu\text{s}$ , therefore their frequency spectra is entirely above 100 kHz;
- the maximum current during the discharge is 9 A (according to power supply limitations);
- the energy released during each spark cannot exceed 2 Joules, as each HV power supply (emitter and accelerator) has a maximum stored energy of 1 J. In fact, as during discharge the voltage drops, the spark is extinguished before the capacitors are fully discharged.

Sparks will also be characterized in terms of electromagnetic disturbance in the frame of the above mentioned EMC tests.

Finally, the EMC disturbance associated with the ion beam can be questioned. Considering the beam current is lower than 1 mA, the magnetic fields the beam can generate are microscopic ( $< 0.4 \text{ nT}$  @ 0.5 m). In addition, the electromagnetic energy associated with ions acceleration, which can be calculated using Larmor's equation, is in the order of  $10^{-19} \text{ W}$ .

## 8.2 Contamination

To avoid direct plume impingement, the thrusters should be mounted at proper angles on the S/C, considering the ion beam divergence reported in sect. 3.5.7.

Due to the fact that the surroundings of the thrusters will anyway experience some contamination by cesium (neutral evaporation and charge-exchange ions), special precautions shall be used in the selection of materials in the close vicinity of the thruster.

In particular, fluorinated plastics (FEP, PTFE, etc.) should be avoided.

Gold-plated surfaces may experience variation of their thermo-optical properties.

Optical surfaces (mirrors, glass windows, IR sensors or star sensors) should be shielded from direct view of thrusters. If this is not possible, and if the surface of the sensitive components is very cold for some reason, it might be necessary to heat it up from time to time to enhance evaporation of cesium that may have condensed on the glass.

If needed, Alta has materials testing capabilities to assess compatibility with cesium in early design phases.

For reference, the following paper reporting investigations performed in the frame of Microscope can be consulted:

- E. Chesta et al., *MICROSCOPE mission phase B propulsion system activities at spacecraft level: requirements consolidation and assessment of neutralization and contamination effects*, IEPC-2007-213, Presented at the 30th International Electric Propulsion Conference, Florence, Italy, September 17-20, 2007

## 9 Design, development and verification plan

### 9.1 Technology Readiness Level

The following table presents the technology readiness level for the proposed solution, detailed down at unit and/or component level, with missing development steps to achieve "Flight Qualified" status (TRL 8):

Unit / element	TRL <sup>(*)</sup>	Level description	Steps to achieve TRL 8
PCU	6	System/subsystem model or prototype demonstration in a relevant environment (ground or space)	- Demonstration of enhanced step response on PCU EBB - Proto-flight qualification of PFM
NA	8	Actual system completed and "Flight qualified" through test and demonstration (ground or space)	None
Thruster Unit	8	Actual system completed and "Flight qualified" through test and demonstration (ground or space)	None
Tank	5	Component and/or breadboard validation in relevant environment	- Measurement of maximum hydrostatic head on EM thruster - Full qualification of tank (QM) - Testing of one full thruster (DM) for functionality
MTC (structure)	6	System/subsystem model or prototype demonstration in a relevant environment (ground or space)	- Design and verification (analysis) of new structure - Proto-flight qualification of PFM

<sup>(\*)</sup> Upon conclusion of Lisa Pathfinder qualification.

**Table 9.1: MTS technology readiness level.**

### 9.2 DDV plan

The following flow diagram shows the proposed design, development and verification plan for the FEEP Micro-Thrusters System for GG.

Draft planning is provided in ALTA/P09-12/FGG.



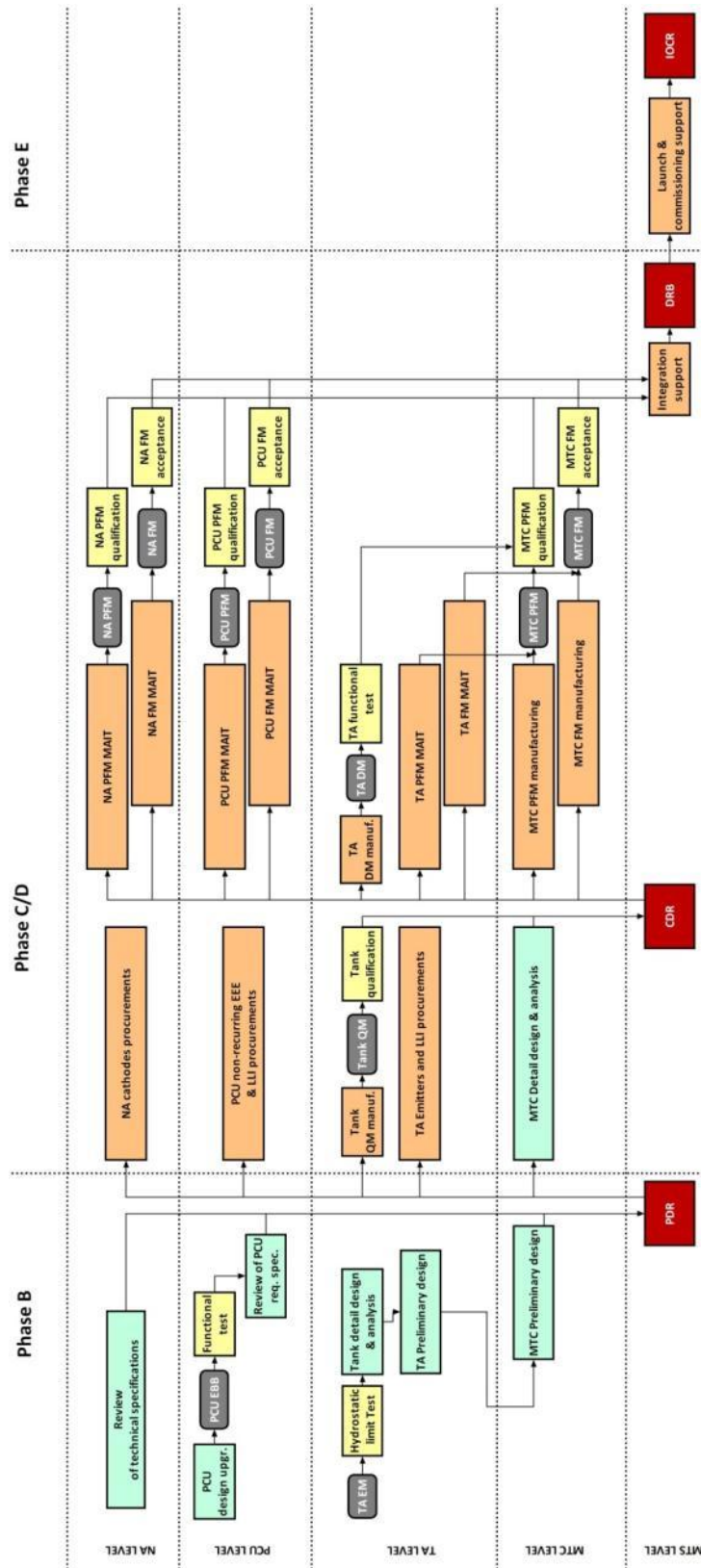


Figure 9.1: Design, Development and Verification Plan (overall).

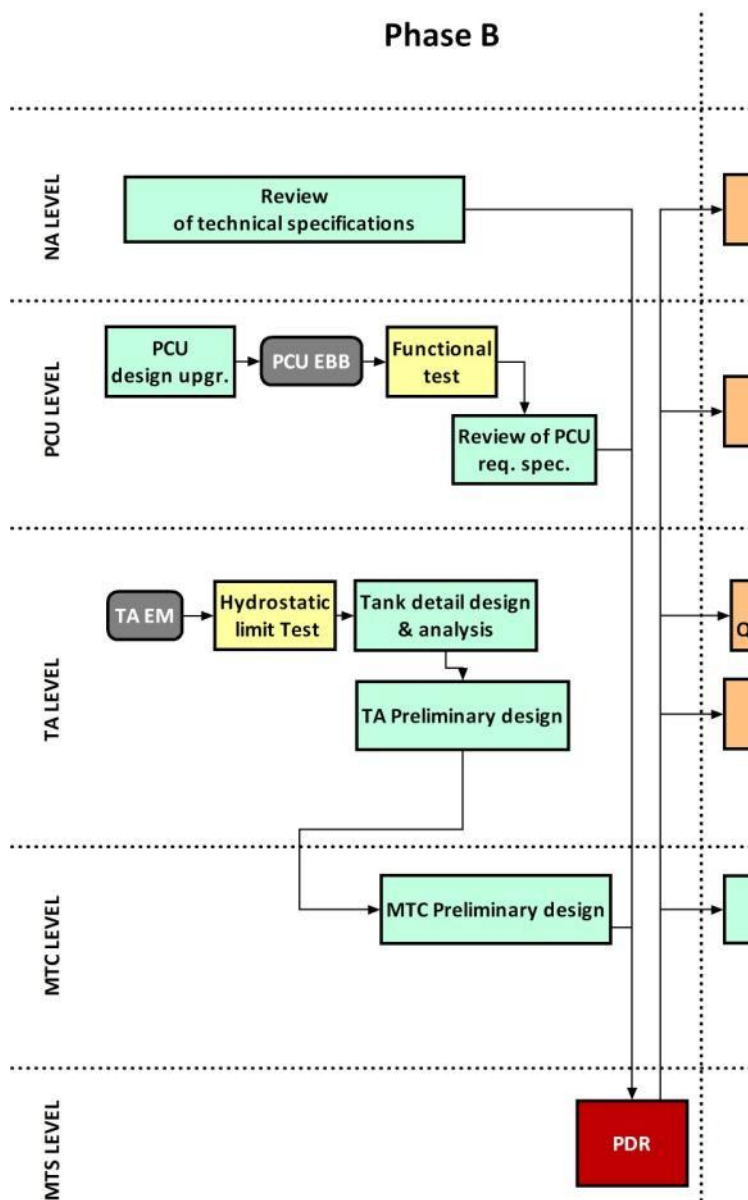


Figure 9.2: Design, Development and Verification Plan (phase B).

### Phase C/D

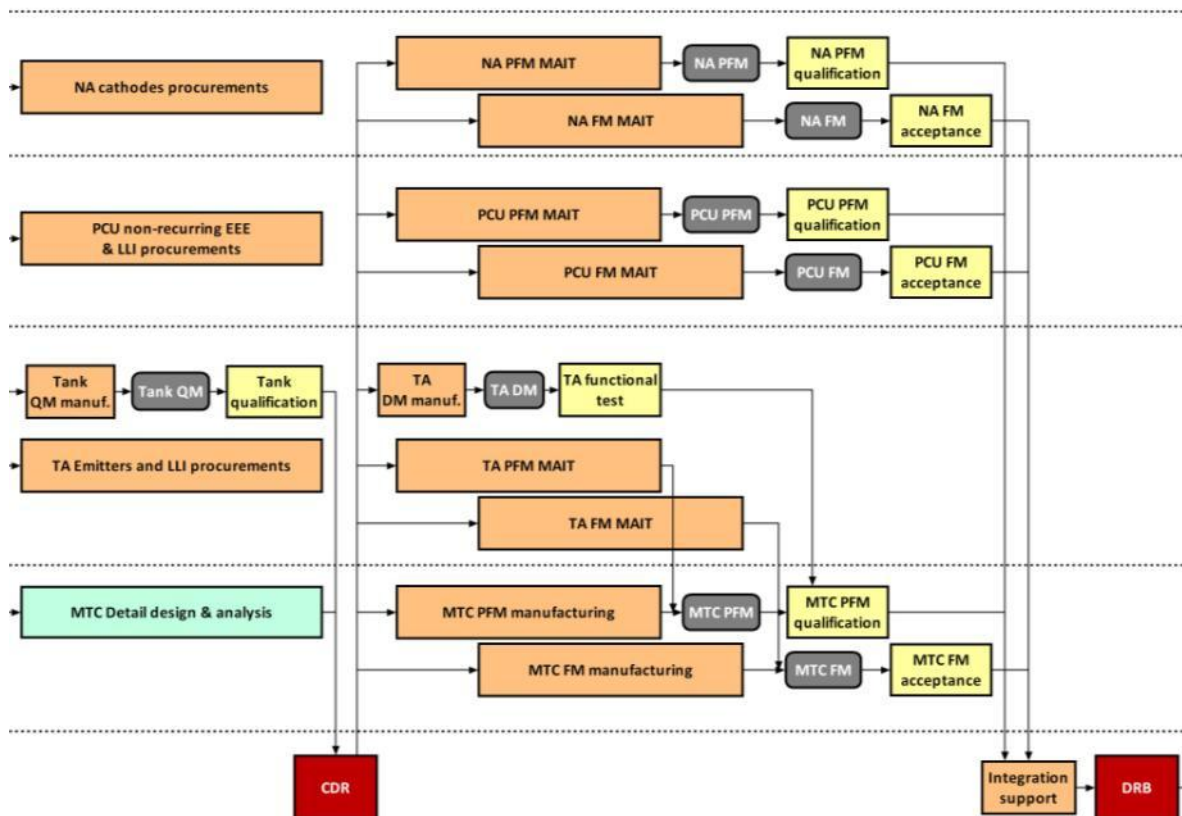


Figure 9.3: Design, Development and Verification Plan (phase C/D).

### Phase E

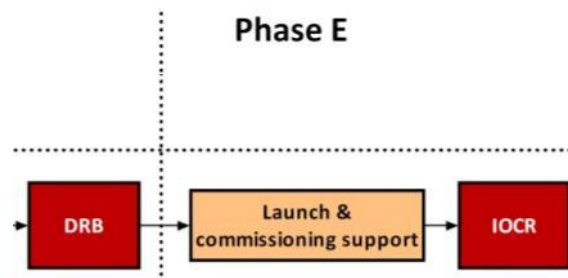


Figure 9.4: Design, Development and Verification Plan (phase E).

## 10 Documents

### 10.1 Applicable Documents

- [AD 1] Deleted.
- [AD 2] “Galileo Galilei Mission Requirement Document”, SD-TN-AI-1167, Issue 1 draft, October 2008
- [AD 3] Experiment Concept and Requirements Document (ERD), SD-TN-AI-1163, Issue 1 draft, October 2008
- [AD 4] “Galileo Galilei System Technical Specification”, SD-SY-AI-0014, January 09, Issue Draft
- [AD 5] “Thrusters requirements (preliminary)”, TAS-I , e-mail 29/02/09

### 10.2 Standards

- [SD 1] ECSS-M-00-02A, Space Project Management – Tailoring of Space Standards, 25 April 2000
- [SD 2] ECSS-E-10 Part 1, System engineering
- [SD 3] ECSS-E-10-02A, Space Engineering – Verification
- [SD 4] ECSS-E-30, Space Engineering - Mechanical - Part 1: Thermal
- [SD 5] ECSS-E-30, Space Engineering - Mechanical - Part 2: Structural
- [SD 6] ECSS-E-30, Space Engineering - Mechanical - Part 3: Mechanism
- [SD 7] ECSS-E-30, Space Engineering - Mechanical - Part 5: Propulsion
- [SD 8] ECSS-E-30, Space Engineering - Mechanical - Part 6: Pyrotechnics
- [SD 9] ECSS-E-30, Space Engineering - Mechanical - Part 7: Mechanical Parts
- [SD 10] ECSS-E-30, Space Engineering - Mechanical - Part 8: Materials
- [SD 11] ECSS-E-40 Part 1, Software Engineering Standards
- [SD 12] ECSS-E-ST-60-10C Control Performance
- [SD 13] ECSS-Q-00A, Space Product Assurance - Policy and Principles, and related Level 2 standards.
- [SD 14] ECSS-Q-ST-70-01C, Cleanliness and contamination control, 15 November 2008

### 10.3 Reference Documents

- [RD 1] GG Phase A Study Report, Nov. 1998, revised Jan. 2000, available at: <http://eotvos.dm.unipi.it/nobili/ggweb/phaseA/index.html>
- [RD 2] Supplement to GG Phase A Study (GG in sun-synchronous Orbit) “Galileo Galilei-GG”: design, requirements, error budget and significance of the ground prototype”, A.M. Nobili et al., Physics Letters A 318 (2003) 172–183, available at the following official website: [http://eotvos.dm.unipi.it/nobili/documents/generalpapers/GG\\_PLA2003.pdf](http://eotvos.dm.unipi.it/nobili/documents/generalpapers/GG_PLA2003.pdf)
- [RD 3] GG.ALT.TN.2001, issue 1, Preliminary information on FEPP.
- [RD 4] GG.ALT.TN.2002, issue 1, Evaluation of Preliminary Thruster Requirements.
- [RD 5] S2-AASI-RP-2001, issue 2, NA Lisa PF Design Report.
- [RD 6] S2-EST-TN-2025, 31/7/08, Analysis of FEPP Arc Discharge.
- [RD 7] S2-AASI-ICD-2001, issue 4, NA Interface Control Document.

## 11 Acronyms

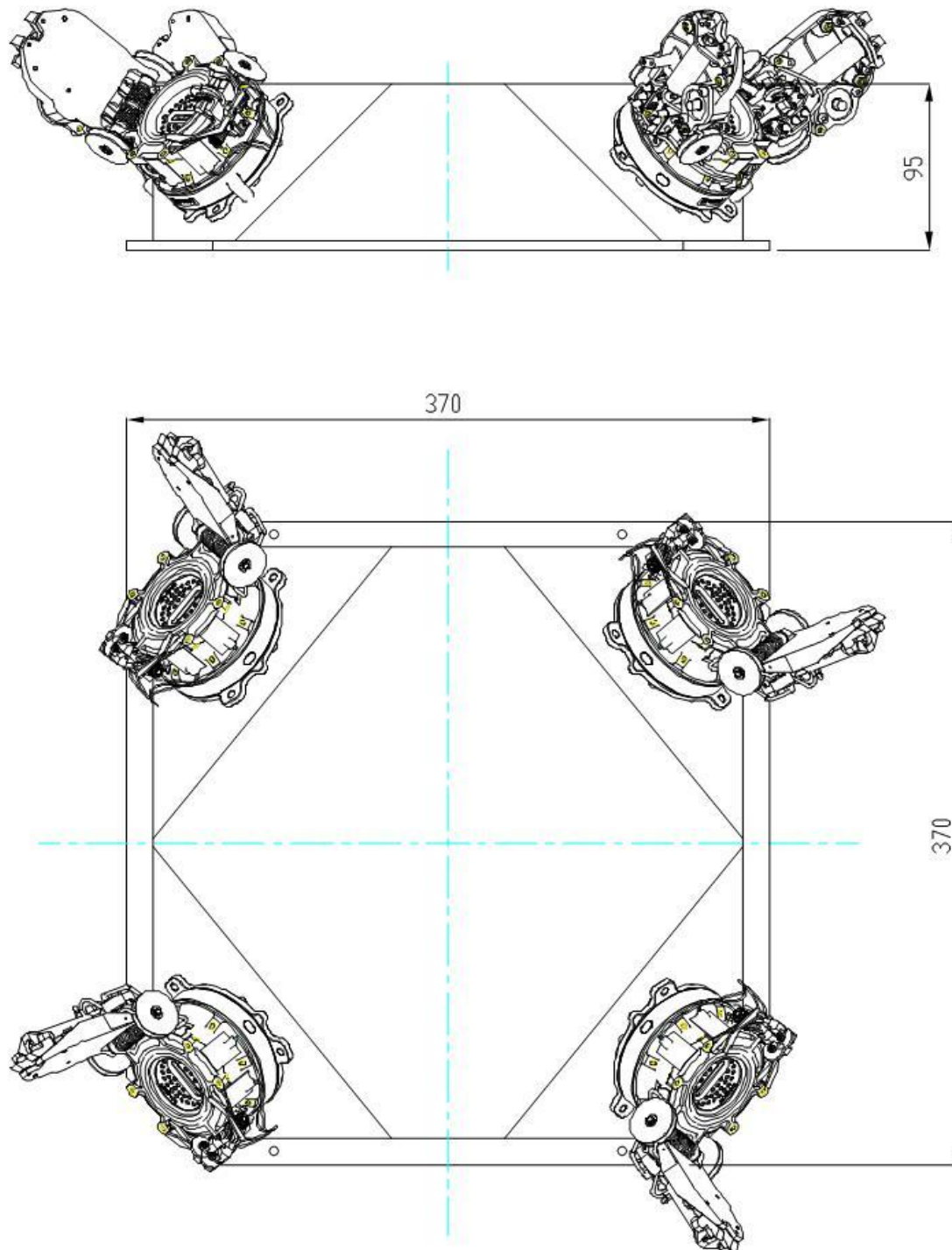
The following acronyms and abbreviations are used within this document.

<b>AD</b>	Applicable Document	<b>MTC</b>	Micro-Thrusters Cluster
<b>AOCS</b>	Attitude and Orbit Control System	<b>MTS</b>	(FEEP) Micro-Thrusters (sub)System
<b>ASI</b>	Agenzia Spaziale Italiana	<b>MTSA</b>	(FEEP) Micro-Thrusters Sub-Assembly
<b>CNES</b>	Centre National d'Etudes Spatiales	<b>N/A</b>	Not Applicable
<b>COM</b>	Centre of Mass	<b>NA</b>	Neutralizer Assembly
<b>DFACS</b>	Drag Free Attitude and Control Subsystem	<b>NASA</b>	National Aeronautics and Space Administration
<b>DRS</b>	Disturbance Reduction System	<b>NU</b>	Neutralizer Unit
<b>DTM</b>	Direct Thrust Measurement	<b>OBC</b>	On-Board Computer
<b>EBB</b>	(PCU) Elegant Breadboard	<b>P/L</b>	Payload
<b>ECSS</b>	European Cooperation for Space Standardisation	<b>PA</b>	Product Assurance
<b>EMC</b>	Electromagnetic Compatibility	<b>PCU</b>	Power Control Unit
<b>EMI</b>	Electromagnetic Interference	<b>PCDU</b>	Power Conditioning and Distribution Unit
<b>EOL</b>	End Of Life	<b>PFM</b>	Proto-Flight Model
<b>EP</b>	Equivalence Principle	<b>PGB</b>	Pico Gravity Box
<b>ESA</b>	European Space Agency	<b>PMD</b>	Propellant Management Device
<b>ESD</b>	Electrostatic Discharge	<b>QL</b>	Qualification Loads
<b>ET</b>	Endurance Test	<b>QM</b>	Qualification Model
<b>FCA</b>	FEEP Cluster Assembly	<b>RD</b>	Reference Document
<b>FEEP</b>	Field Emission Electric Propulsion	<b>RFI</b>	Request for Information
<b>FEM</b>	Finite Element Model	<b>RFQ</b>	Request for Quotation
<b>FOS</b>	Factor of Safety	<b>S/C</b>	Spacecraft
<b>G/S</b>	Ground Station	<b>S/S</b>	Subsystem
<b>GA</b>	Galileo Avionica S.p.A.	<b>SoW</b>	Statement of Work
<b>GG</b>	Galileo Galilei	<b>SPoF</b>	Single Point of Failure
<b>HK</b>	Housekeeping	<b>SPRF</b>	Satellite Physical Reference Frame
<b>HV</b>	High Voltage	<b>STS</b>	System Technical Specification
<b>I/F</b>	Interface	<b>TA</b>	Thruster Assembly
<b>Isp</b>	Specific Impulse	<b>TAPT</b>	Thruster Assembly Priming Test
<b>ITAR</b>	International Traffics in Arms Regulations	<b>TAS-I</b>	Thales Alenia Space - Italia
<b>LEOP</b>	Launch and Early Orbit Phase	<b>TBC/tbc</b>	To be confirmed
<b>LISA</b>	Laser Interferometer Space Antenna	<b>TBD/tbd</b>	To be defined
<b>LL</b>	Limit Loads	<b>TC</b>	Telecommand
<b>LOM</b>	Lid-Opening Mechanism	<b>TM</b>	Telemetry
<b>LPF</b>	Lisa Pathfinder	<b>TRP</b>	Temperature Reference Point
<b>MLI</b>	Multi Layer Insulation	<b>TSD</b>	Tank Sealing Device
<b>MPS</b>	Micro Propulsion System	<b>TU</b>	Thruster Unit
<b>MRD</b>	Mission Requirement Document		



## Appendix A Drawings

### A.1 MTC envelope dimensions







## Appendix B

### B.1 Mass budget

Unit	Mass including margin	Remarks
Micro-Thrusters Cluster	7.3 kg	Including 4 Thruster Assemblies
Neutralizer Assembly	0.5 kg	Including 2 Neutralizer Units
PCU + harness	5.7 kg	Including HV connection box
<b>Total MTSA</b>	<b>13.5 kg</b>	
<b>Total Option A (2 MTSA)</b>	<b>27 kg</b>	
<b>Total Option B (3 MTSA)</b>	<b>40.5 kg</b>	

Table B.1: Preliminary MTS mass budget.

### B.2 Power budget

PCU Status	Thrust level ( $\mu\text{N}$ )	Power consumption (W)			Total PCU input power (W)	Remarks
		MTC	NA	PCU + harness		
SB	-	-	-	5.8	5.8	Only PCU on
T	0	4.2	5.8	31.5	41.5	Neutralizer on., thrusters ready to fire.
T	4x10	6.2	5.8	31.9	43.9	Neutralizer on., 4 thrusters firing at 10 $\mu\text{N}$ .
T	4x60	16.4	5.8	33.8	56.0	Neutralizer on., 4 thrusters firing at 60 $\mu\text{N}$ .
T	4x150	36.3	5.8	37.6	79.7	Neutralizer on., 4 thrusters firing at 150 $\mu\text{N}$ .

Table B.2: Preliminary MTSA power budget, BOL conditions.

PCU Status	Thrust level ( $\mu\text{N}$ )	Power consumption (W)			Total PCU input power (W)	Remarks
		MTC	NA	PCU + harness		
SB	-	-	-	5.8	5.8	Only PCU on
T	0	25.6	5.8	31.3	62.7	Neutralizer on., thrusters ready to fire.
T	4x10	28.4	5.8	31.7	65.9	Neutralizer on., 4 thrusters firing at 10 $\mu\text{N}$ .
T	4x60	43.8	5.8	33.8	83.4	Neutralizer on., 4 thrusters firing at 60 $\mu\text{N}$ .
T	4x150	76.6	5.8	38.0	120.4	Neutralizer on., 4 thrusters firing at 150 $\mu\text{N}$ .

Table B.3: Preliminary MTSA power budget, EOL conditions.

End of document